Electronic Supplementary Material (ESI) for New Journal of Chemistry.

Supporting Information

Neat and Rapid Preparation of Hydrophobic Magnetic Ionic Liquids Composed of Transition Metal Chelates Featuring *In-situ* Formation Capabilities in Aqueous Matrices

Nabeel Mujtaba Abbasi,[1] Pravin S. Shinde,[2] Kathryn E. O'Harra,[2] Anis Biswas,[1] Jason E. Bara,[2] and Jared L. Anderson[1,*]

[1]Department of Chemistry, Iowa State University, Ames, Iowa 50011, USA and [2]Department of Chemical & Biological Engineering, University of Alabama, Tuscaloosa, AL 35487-0203 USA

List of chemicals and reagents

Triethylamine (Et_3N, 99%) was purchased from Acros Organics (Morris Plains, NJ, USA). Hydrochloric acid (HCl, certified ACS plus), 1-(3-aminopropyl)imidazole (AmIm, 98%), sodium hydrogen carbonate ($NaHCO_3$, certified ACS powder, 99.7-100.3%), cobalt(II) carbonate ($CoCO_3$, 99% metal basis), *N*,*N*-dimethylacetamide (*N*,*N*-DMAc, 99%), and ammonium hydroxide (NH_4OH, certified ACS plus) were purchased from Fisher Scientific (Pittsburgh, PA, USA). Nickel(II) carbonate ($NiCO_3$, 99%) was obtained from Oakwood Chemical. Diglycolyl chloride (> 97%), *N*,*N*-dimethylpropionamide (*N*,*N*-DMP, 98%), and bis(trifluoromethanesulfonyl)imide ($HNTf_2$, > 99%) were purchased from Tokyo Chemical Industry (TCI, Portland, OR, USA). 1-Hexylimidazole (Him, 95%) and 1-octyl-1H-imidazole (OIm, 96%) were procured from Ambeed. Diethyl ether (≥ 99%) and dioctylamine (97%) were purchased from MilliporeSigma (St. Louis, MO, USA).

Magnetic susceptibilities and calculations for the effective magnetic moment (μ_{eff}) using MSB

To calculate the molar magnetic susceptibility (X_M), equation 1 was employed.[1]

$$X_M = [C_{bal} L\, M\, (R - R_0)] / (10^9\, m) \quad (1)$$

In equation 1, C_{bal} represents the balance calibration constant, L the length of MIL in the sample tube, M the molecular weight of the solvent, R the instrument reading displayed for the MIL in the sample tube, R_0 the initial reading for the empty tube, and m the mass of the MIL sample. The X_M value can be used to calculate the μ_{eff} using equation 2.[1]

$$\mu_{eff} = 2.83\, (X_M\, T)^{0.5} \quad (2)$$

In equation 2, T represents the temperature at which the magnetic susceptibility measurements were conducted.

Instrument parameters used to obtain TGA and DSC thermograms

To perform TGA measurements, MIL samples (6 – 15 mg) were placed in a high-purity cylindrical alumina pan and heated from 30 to 600 °C at a ramp rate of 10 °C min^{-1} under a constant flow of ultra-high purity argon gas (UHP300, Airgas) at a flow rate of 10 mL min^{-1}. To conduct DSC measurements, samples were prepared by sealing an appropriate amount of MIL using Alodined Hermetic Tzero Aluminum Pan and Hermetic Tzero Lid with the help of a Tzero press. Samples were heated from -40 to 200 °C at a ramp rate of 10 °C min^{-1} and held for 5 min under a steady flow of N_2 gas (20 mL min^{-1}) before being cooled at the same rate.

Crystal structures of hydrated transition metal-based $[NTf_2^-]_2$ salts

In an effort to describe the arrangement of atoms in their crystal lattice, both the $[Co(H_2O)_6][NTf_2]_2$ and $[Ni(H_2O)_6][NTf_2]_2$ salts were examined using X-ray diffraction (XRD). All measurements were performed by employing a monochromatic Cu Kα radiation (λ = 1.5405 Å) in a Bragg-Brentano configuration, covering a 2θ range from 10 to 50° with a step size of 0.004° and dwell time of 5 s per step. During optimization, quick XRD scans (2θ: 5-100°) were performed at step size of 0.02° and dwell time of 1 s per step to narrow down the range for slow scan, as shown in Figure S1. To ensure accuracy, high-purity silicon powder was used as standard reference material.

An overlay of XRD patterns for the hydrated $[NTf_2^-]$ salts of Co^{2+} and Ni^{2+} are provided in Figure S2. XRD patterns of both the salts are almost identical with the notable exception of a few additional peaks around 15, 17.7, and 23° evident for the Co^{2+} salt. The lattice spacing (*d)*-values calculated from Bragg's law for three major high-intensity peaks of Co^{2+} and Ni^{2+} salts were found to be 0.5587, 0.4516, and 0.3771 nm (2θ: 15.85, 19.64, and 23.57°), and 0.5577, 0.5016, and 0.4484 nm (2θ: 15.88, 17.67, and 19.78°), respectively. Although both salts exhibited polycrystalline features, the Ni^{2+} version produced high intensity peaks, demonstrating higher scattering power of its crystal lattice. Additionally, some of the peaks in the XRD scan for the Ni^{2+} salt generated a slight shift towards higher 2θ angles by approximately 0.2°, which can be attributed to the lattice stress stemming from slightly different ionic sizes of Co (0.072 nm) and Ni^{2+} (0.078 nm) cations.

Table S1. Melting point (T_m) /glass transition (T_g) temperatures of MILs as measured by Discovery DSC-250 instrument.

MIL	T_g (°C)	T_m (°C)
[Co(HIm)$_6$][NTf$_2$]$_2$	-	-
[Ni(HIm)$_6$][NTf$_2$]$_2$	-	-
[Co(OIm)$_6$][NTf$_2$]$_2$	-	20.89
[Ni(OIm)$_6$][NTf$_2$]$_2$	-	26.06
[Co(AmIm)$_6$][NTf$_2$]$_2$	-	-
[Ni(AmIm)$_6$][NTf$_2$]$_2$	-	-
[Co(*N*,*N*-DMAc)$_6$][NTf$_2$]$_2$	-	-
[Ni(*N*,*N*-DMAc)$_6$][NTf$_2$]$_2$	-	-
[Co(*N*,*N*-DMP)$_6$][NTf$_2$]$_2$	-	-
[Ni(*N*,*N*-DMP)$_6$][NTf$_2$]$_2$	-	-
[Co(TODGA)$_2$][NTf$_2$]$_2$	-	-
[Ni(TODGA)$_2$][NTf$_2$]$_2$	-	-
[Co(H$_2$O)$_6$][NTf$_2$]$_2$ salt	31.93, 59.93	65.78, 95.04
[Ni(H$_2$O)$_6$][NTf$_2$]$_2$ salt	11.38	74.46

"-" No T_m/T_g peak was observed/reported down to -40 °C

XRD patterns of [NTf_2^-] salts

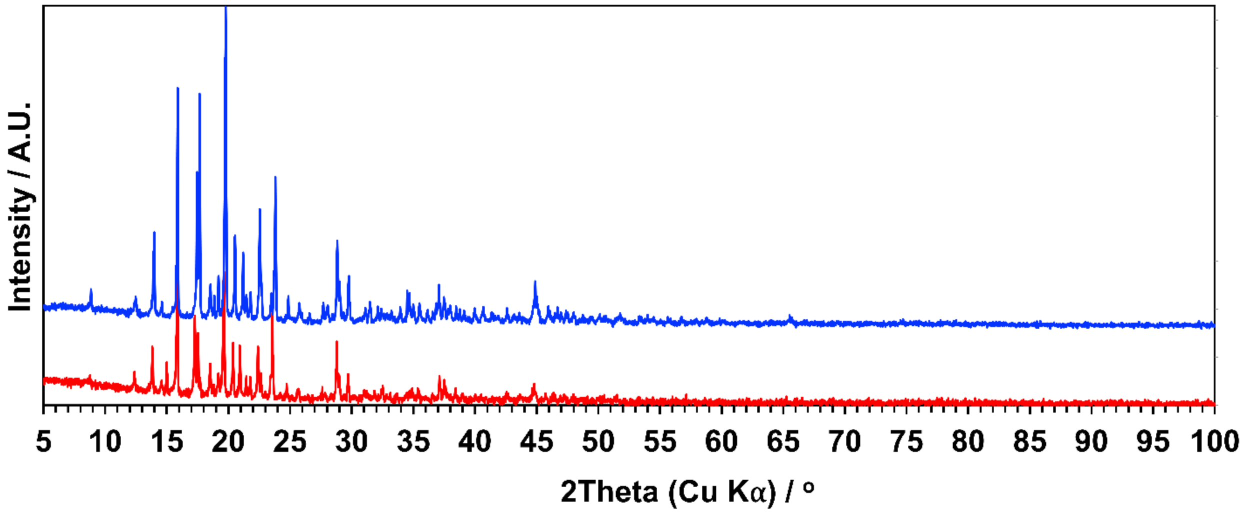

Figure S1: Plot of quick XRD scans for the [NTf_2^-] salts of Co^{2+} and Ni^{2+}. [$Co(H_2O)_6$][NTf_2]$_2$ (——) and [$Ni(H_2O)_6$][NTf_2]$_2$ (——). Parameters: 2θ range from 5 to 100°, step size of 0.02°, and dwell time of 1 s per step.

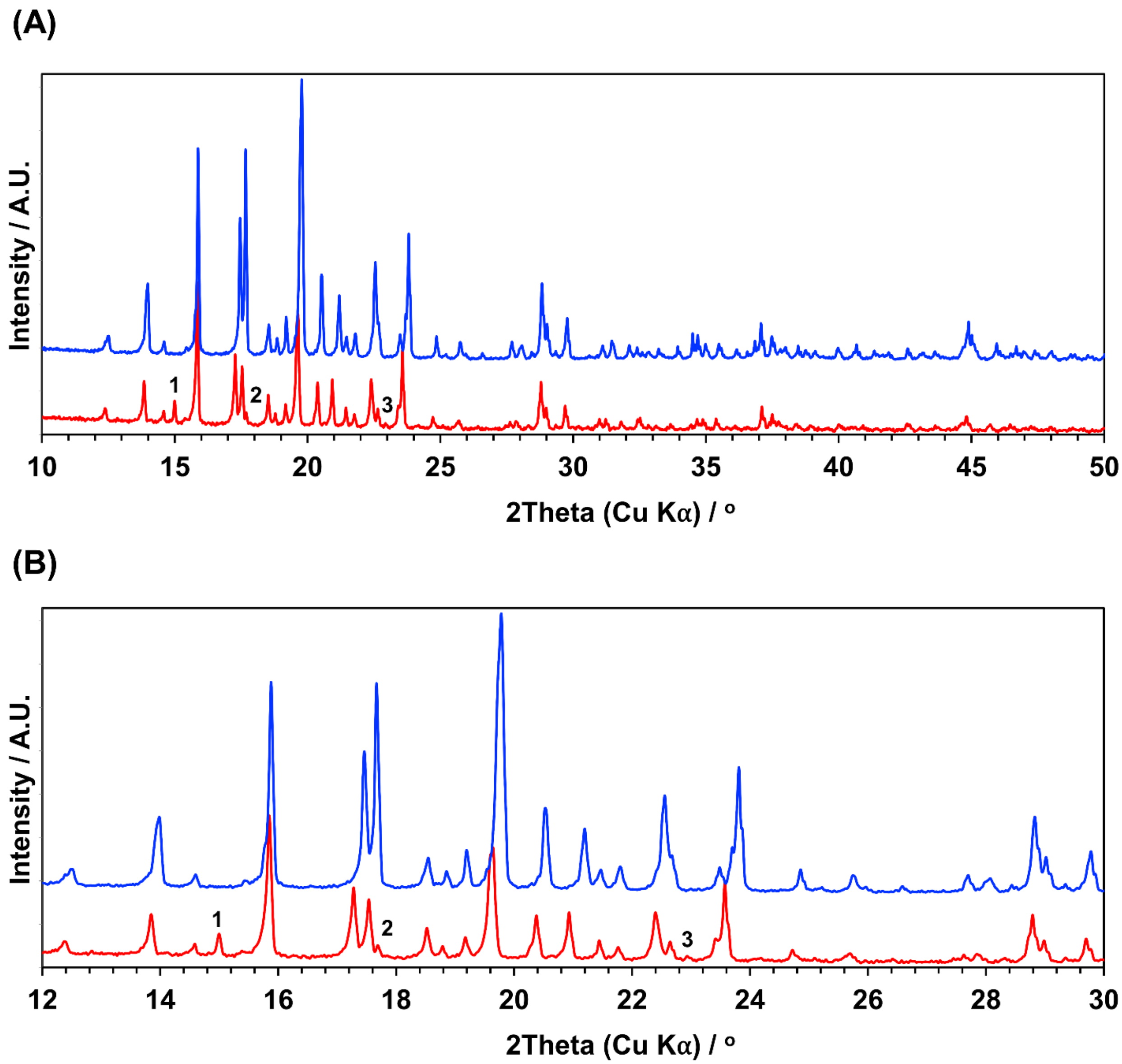

Figure S2: XRD patterns obtained for the [NTf$_2^-$] salts of Co^{2+} and Ni^{2+}. [Co(H_2O)$_6$][NTf$_2$]$_2$ (——) and [Co(H_2O)$_6$][NTf$_2$]$_2$ (——). Parameters: (A) *2θ* range from 10 to 50° and (B) 12 to 30°, step size of 0.004°, and dwell time of 5 s per step. Additional peaks observed for the Co^{2+} salt: **1**, 15°; **2**, 17.7°; and **3**, 23°.

Long-term chemical stability of MILs

Figure S3: Photograph depicting the $[Co(HIm)_6][NTf_2]_2$ MIL sample stored under water for over 6 months.

Magnetization data for transition metal-based MIL measured using SQUID magnetometer

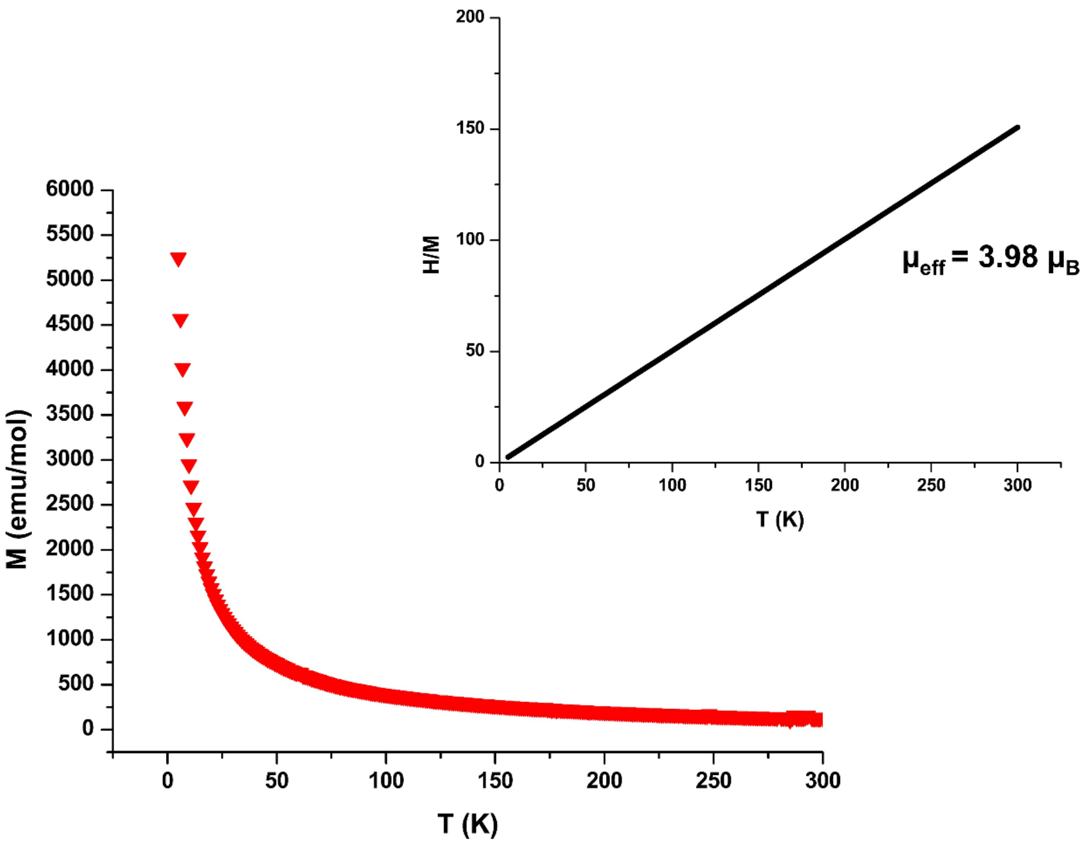

Figure S4: Magnetization of the $[Co(HIm)_6][NTf_2]_2$ MIL as a function of temperature in an applied magnetic field of H = 20 kOe. The inset shows the linear portion of the reciprocal susceptibility vs. temperature curve following Curie-Weiss law.

Thermograms obtained using TGA for transition metal-based MILs

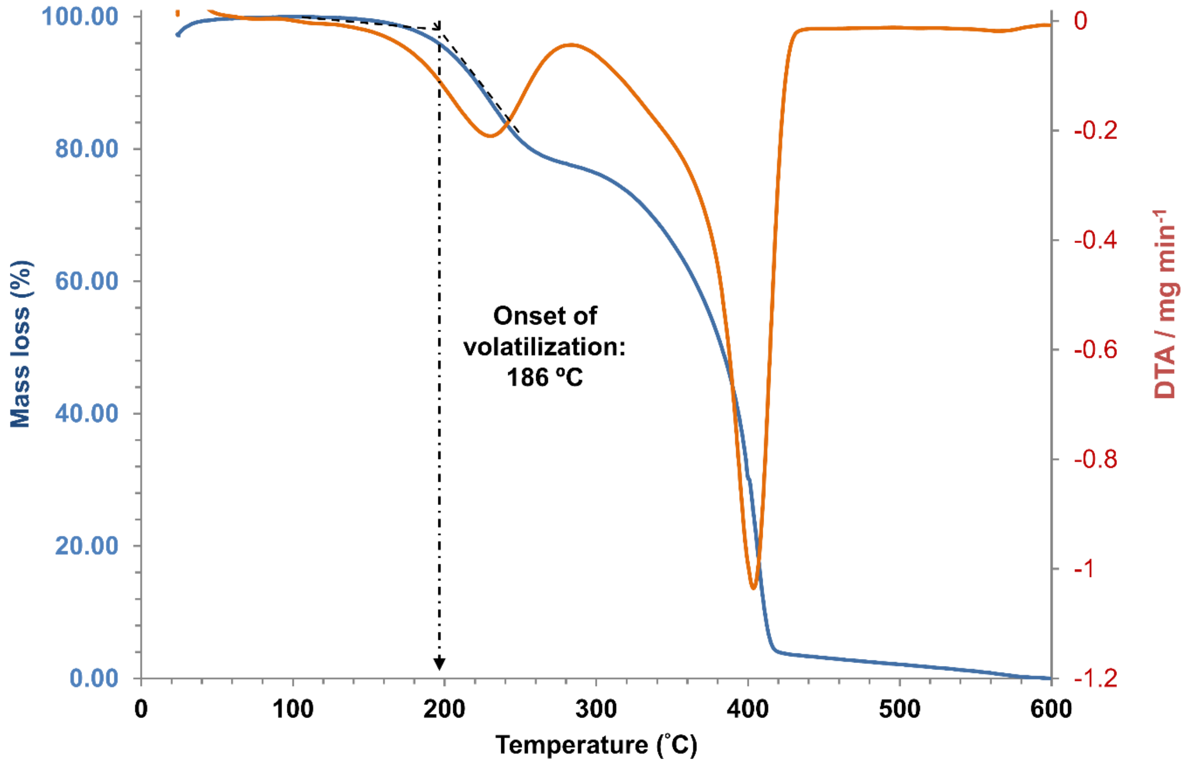

Figure S5: Volatilization/degradation of the $[Co(HIm)_6][NTf_2]_2$ MIL as a function of temperature measured using TGA.

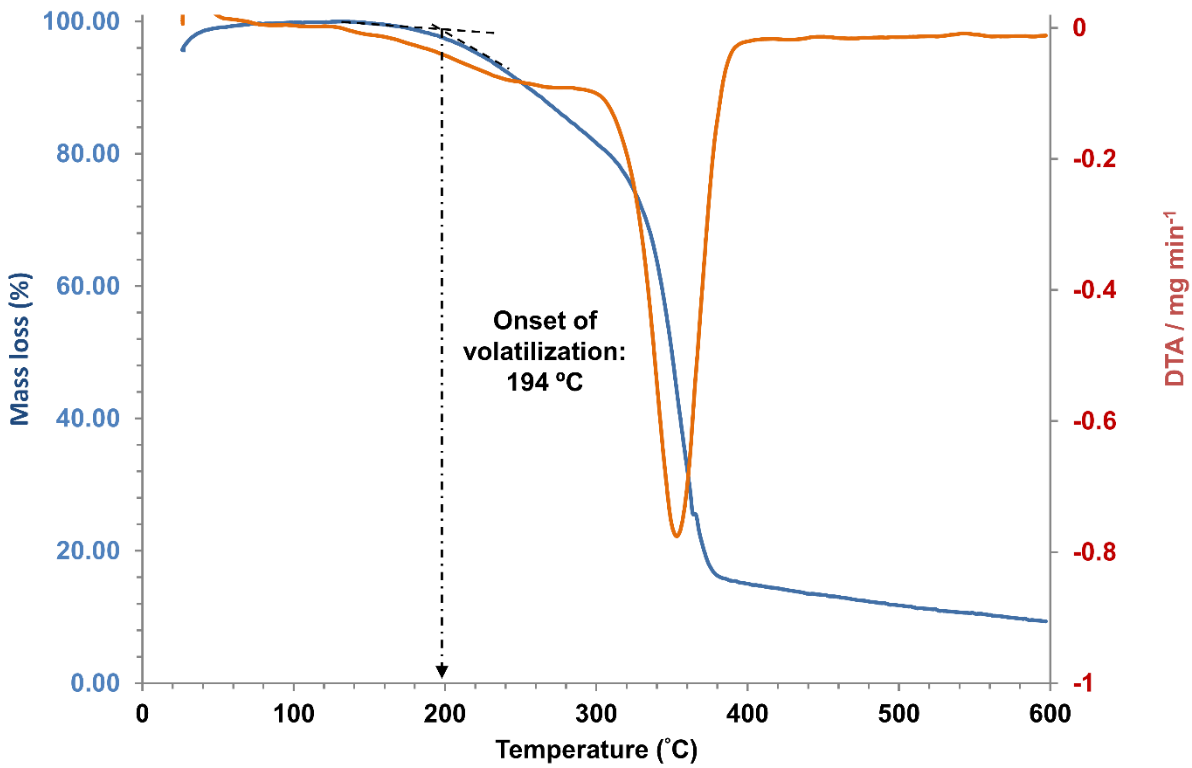

Figure S6: Volatilization/degradation of the $[Ni(HIm)_6][NTf_2]_2$ MIL as a function of temperature measured using TGA.

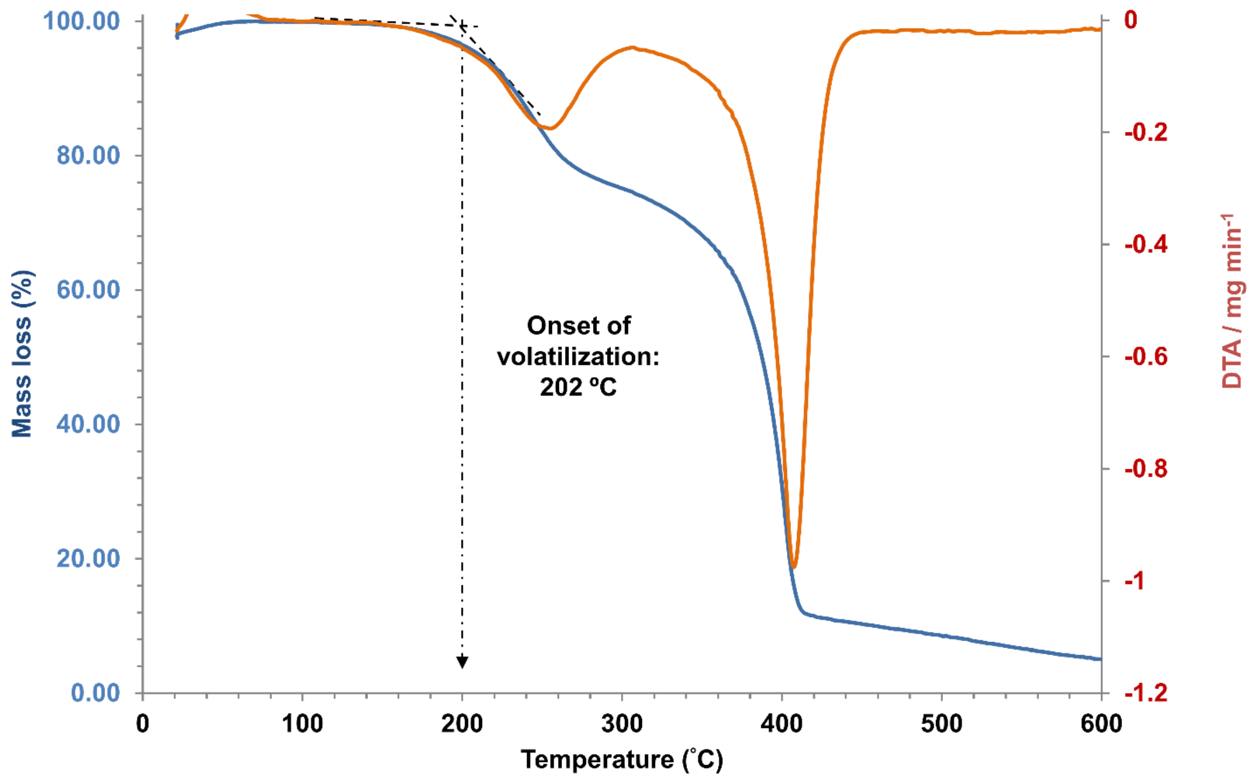

Figure S7: Volatilization/degradation of the $[Co(OIm)_6][NTf_2]_2$ MIL as a function of temperature measured using TGA.

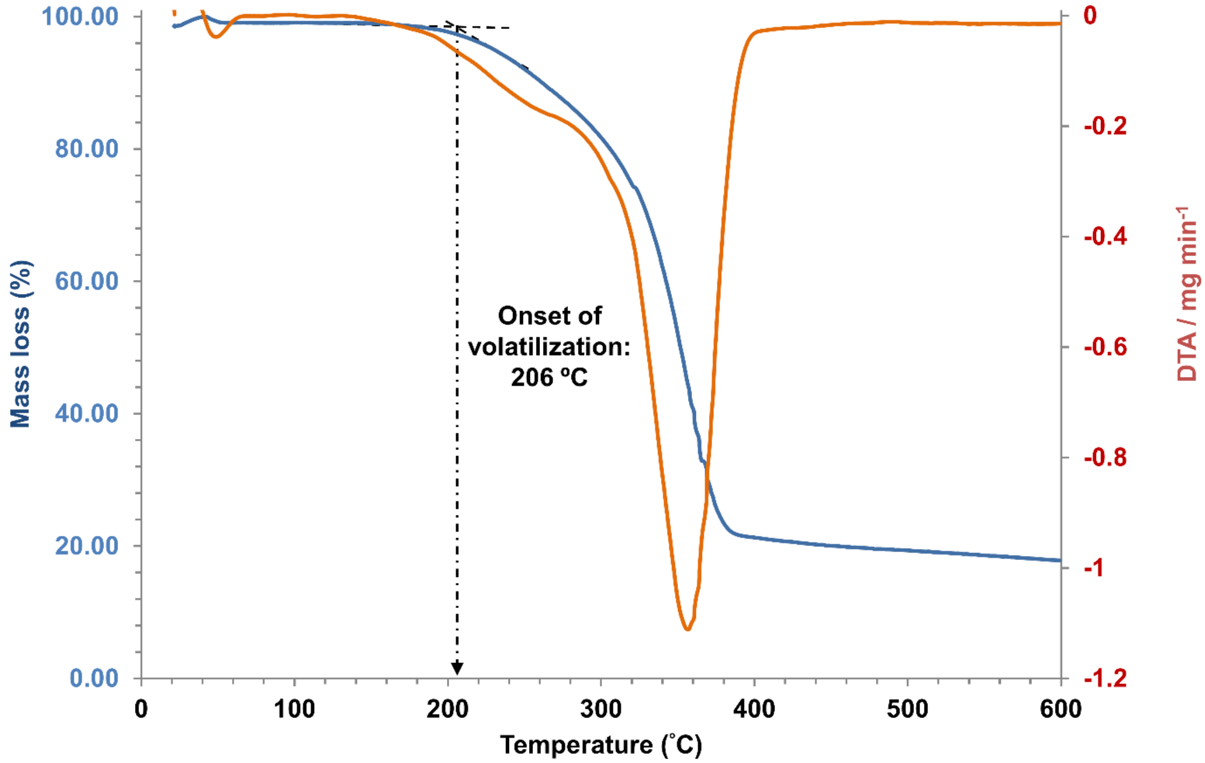

Figure S8: Volatilization/degradation of the $[Ni(OIm)_6][NTf_2]_2$ MIL as a function of temperature measured using TGA.

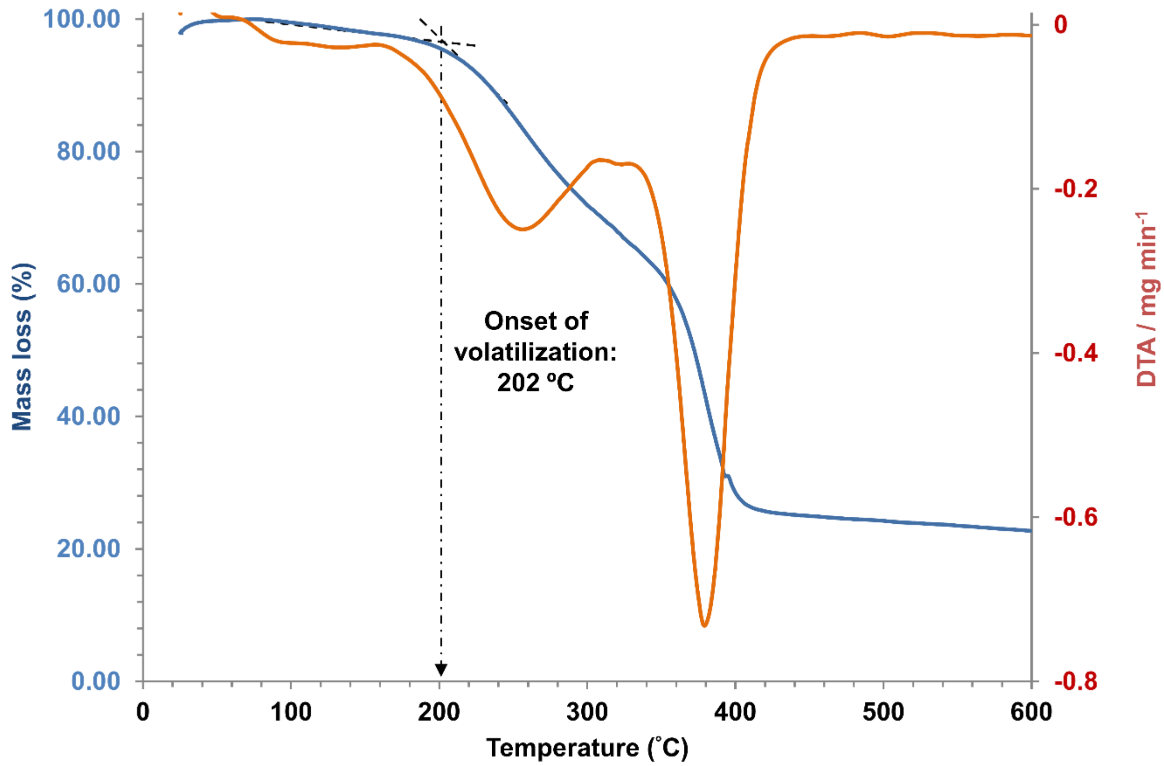

Figure S9: Volatilization/degradation of the [Co(AmIm)$_6$][NTf$_2$]$_2$ MIL as a function of temperature measured using TGA.

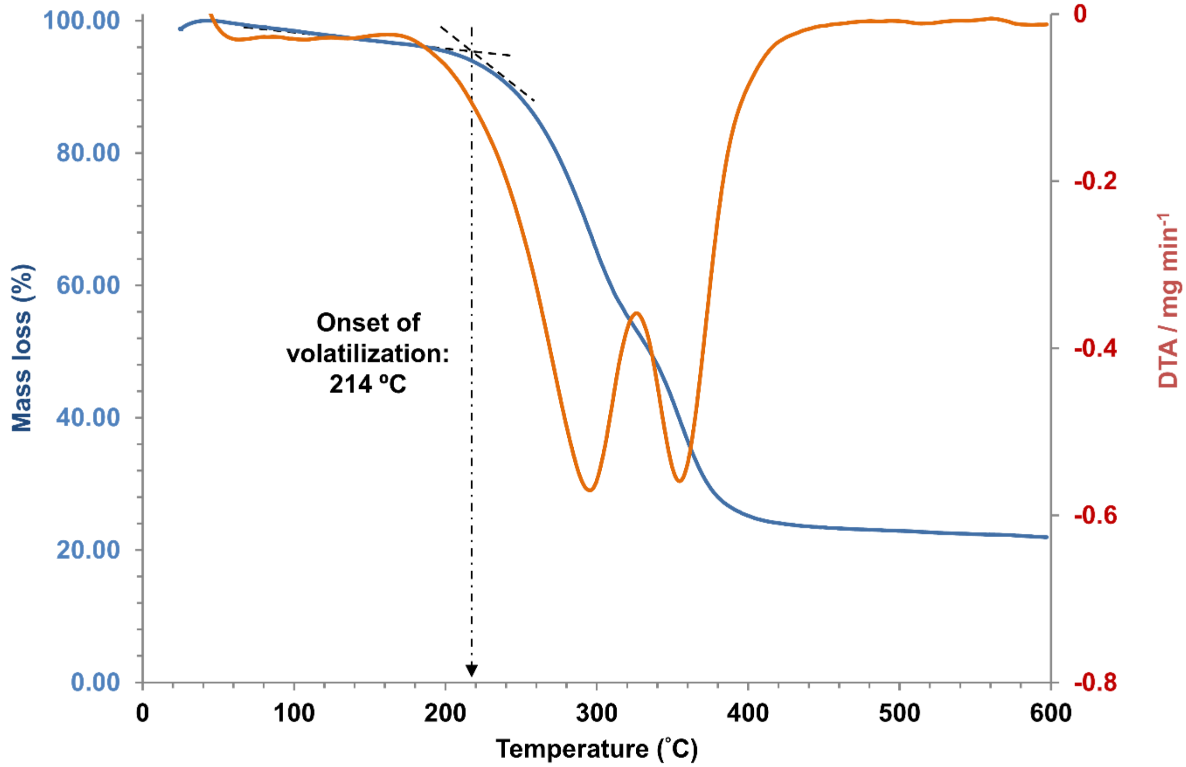

Figure S10: Volatilization/degradation of the [Ni(AmIm)$_6$][NTf$_2$]$_2$ MIL as a function of temperature measured using TGA.

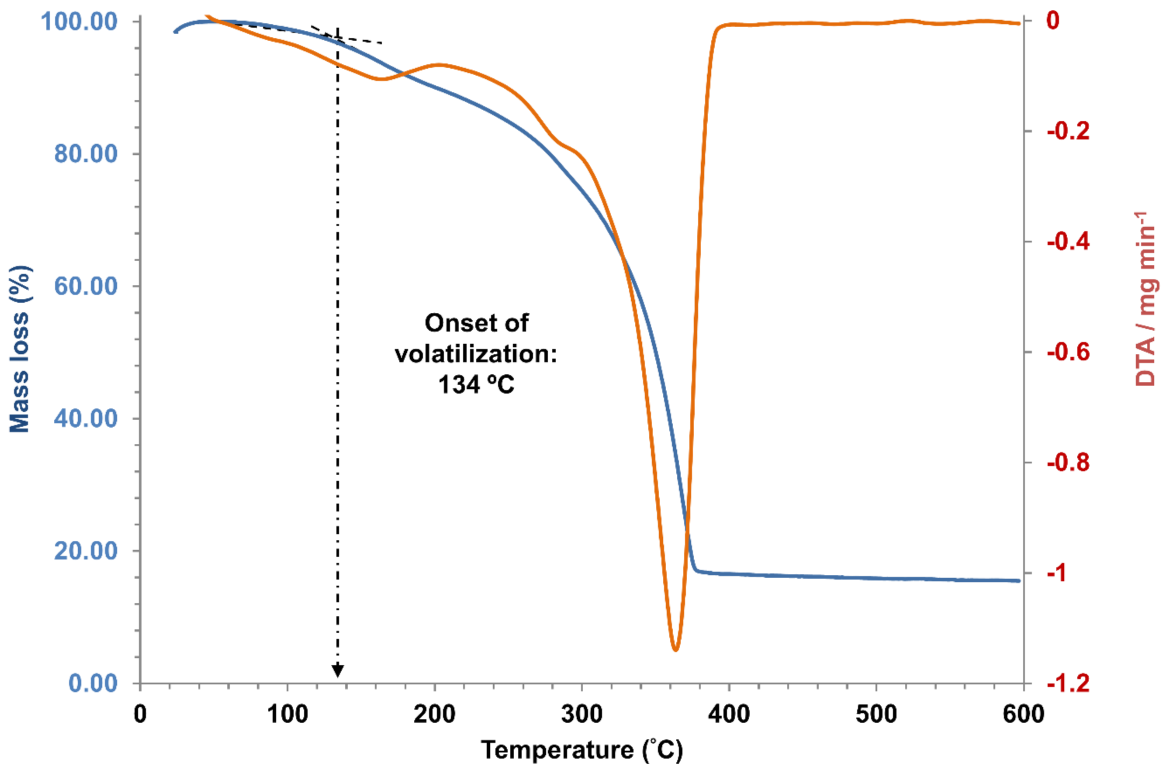

Figure S11: Volatilization/degradation of the [Co(*N*,*N*-DMAc)$_6$][NTf$_2$]$_2$ MIL as a function of temperature measured using TGA.

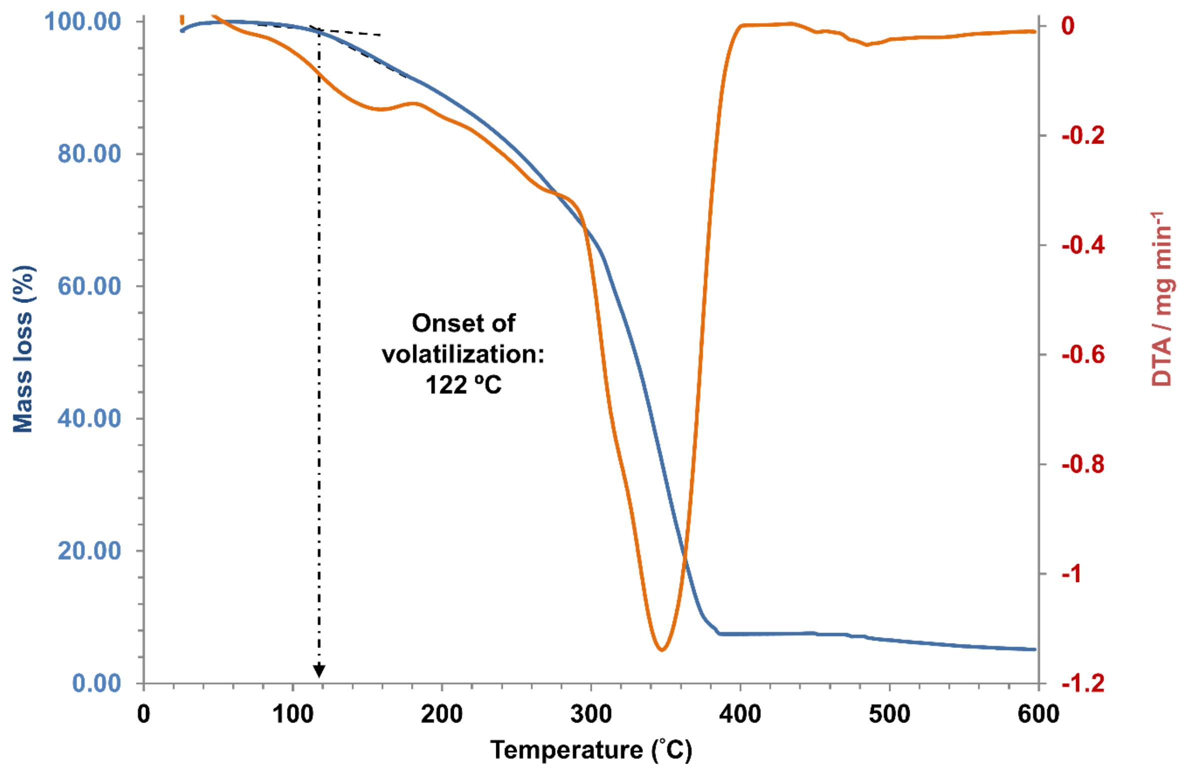

Figure S12: Volatilization/degradation of the [Ni(*N*,*N*-DMAc)$_6$][NTf$_2$]$_2$ MIL as a function of temperature measured using TGA.

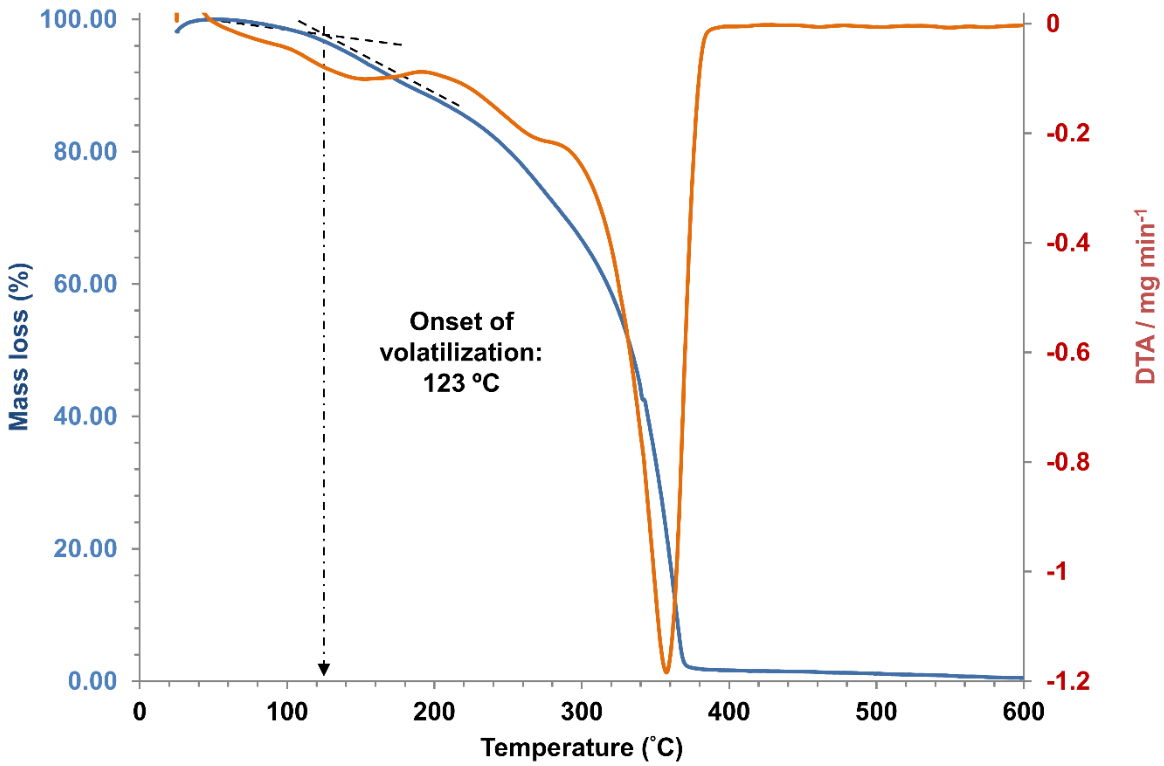

Figure S13: Volatilization/degradation of the [Co(*N*,*N*-DMP)$_6$][NTf$_2$]$_2$ MIL as a function of temperature measured using TGA.

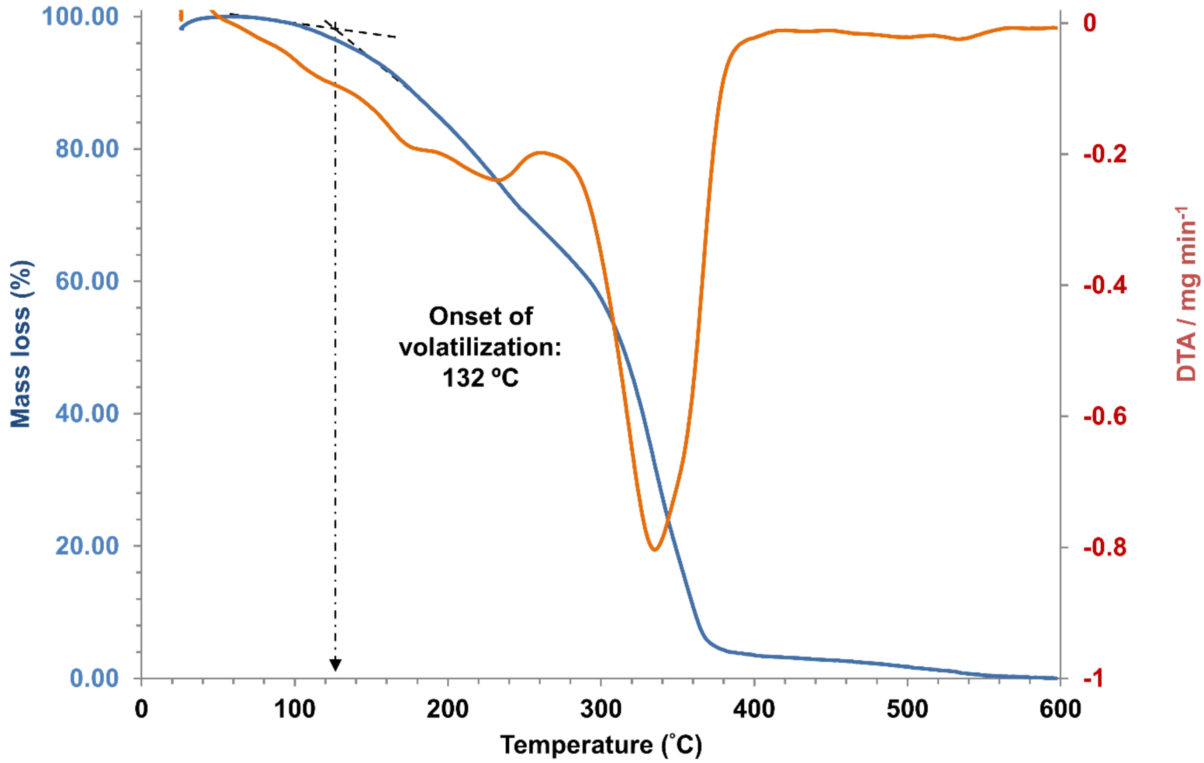

Figure S14: Volatilization/degradation of the [Ni(N,N-DMP)$_6$][NTf$_2$]$_2$ MIL as a function of temperature measured using TGA.

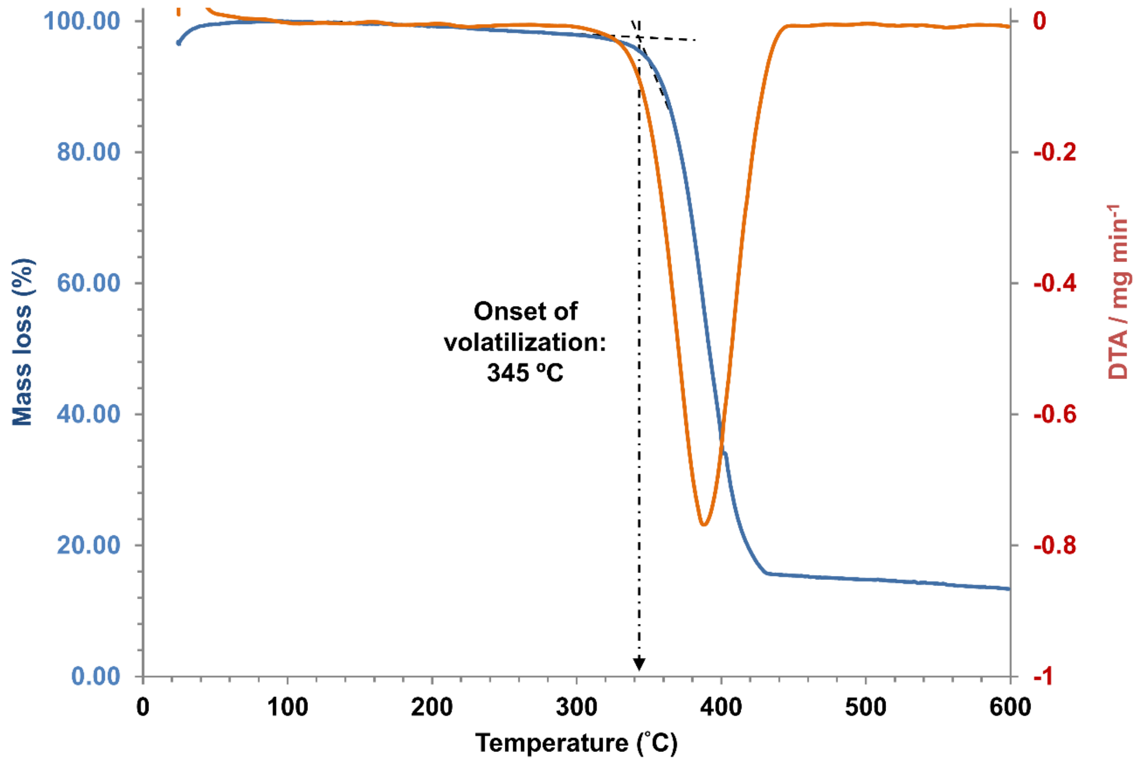

Figure S15: Volatilization/degradation of the $[Co(TODGA)_2][NTf_2]_2$ MIL as a function of temperature measured using TGA.

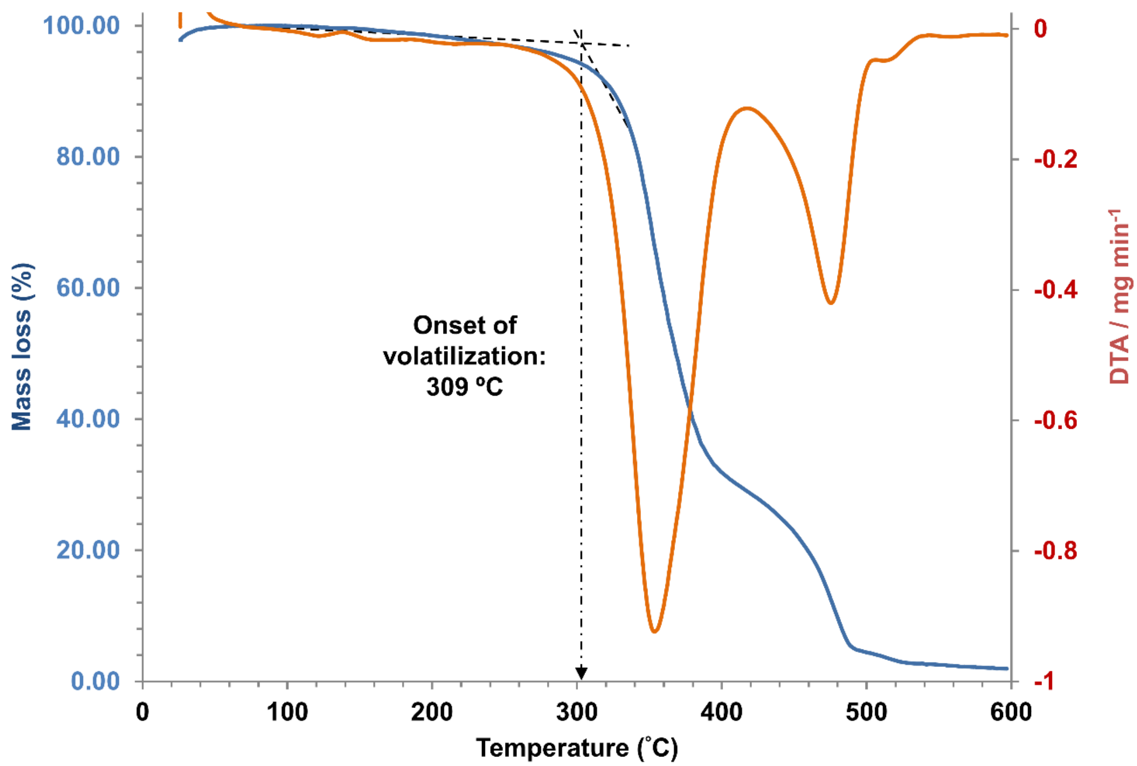

Figure S16: Volatilization/degradation of the $[Ni(TODGA)_2][NTf_2]_2$ MIL as a function of temperature measured using TGA.

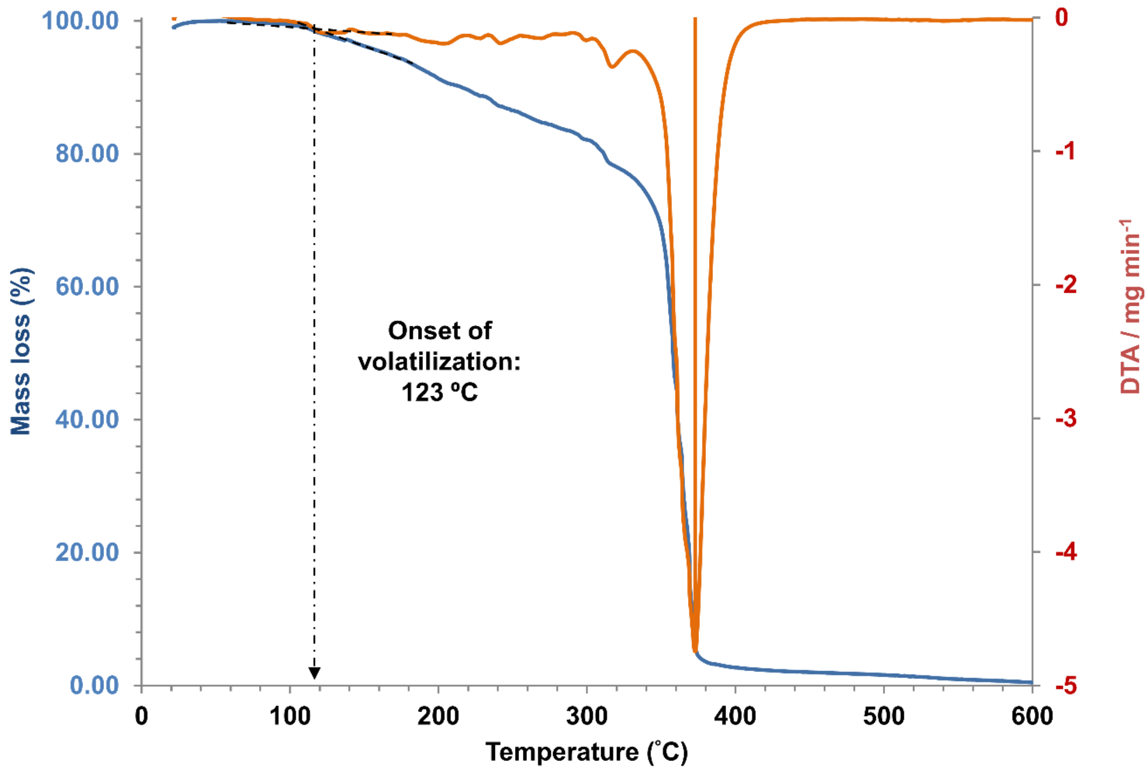

Figure S17: Volatilization/degradation of the $[Co(H_2O)_6][NTf_2]_2$ salt as a function of temperature measured using TGA.

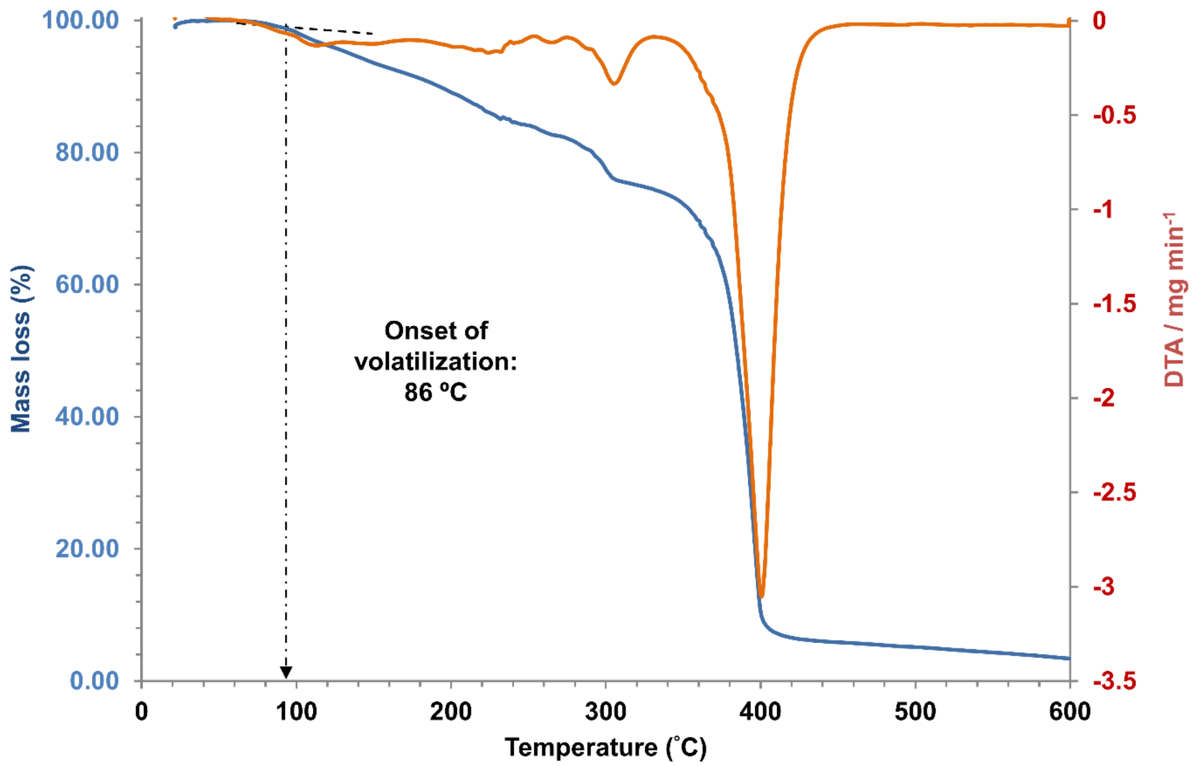

Figure S18: Volatilization/degradation of the $[Ni(H_2O)_6][NTf_2]_2$ salt as a function of temperature measured using TGA.

Thermograms obtained using DSC for MILs comprised of [NTf_2^-] salts

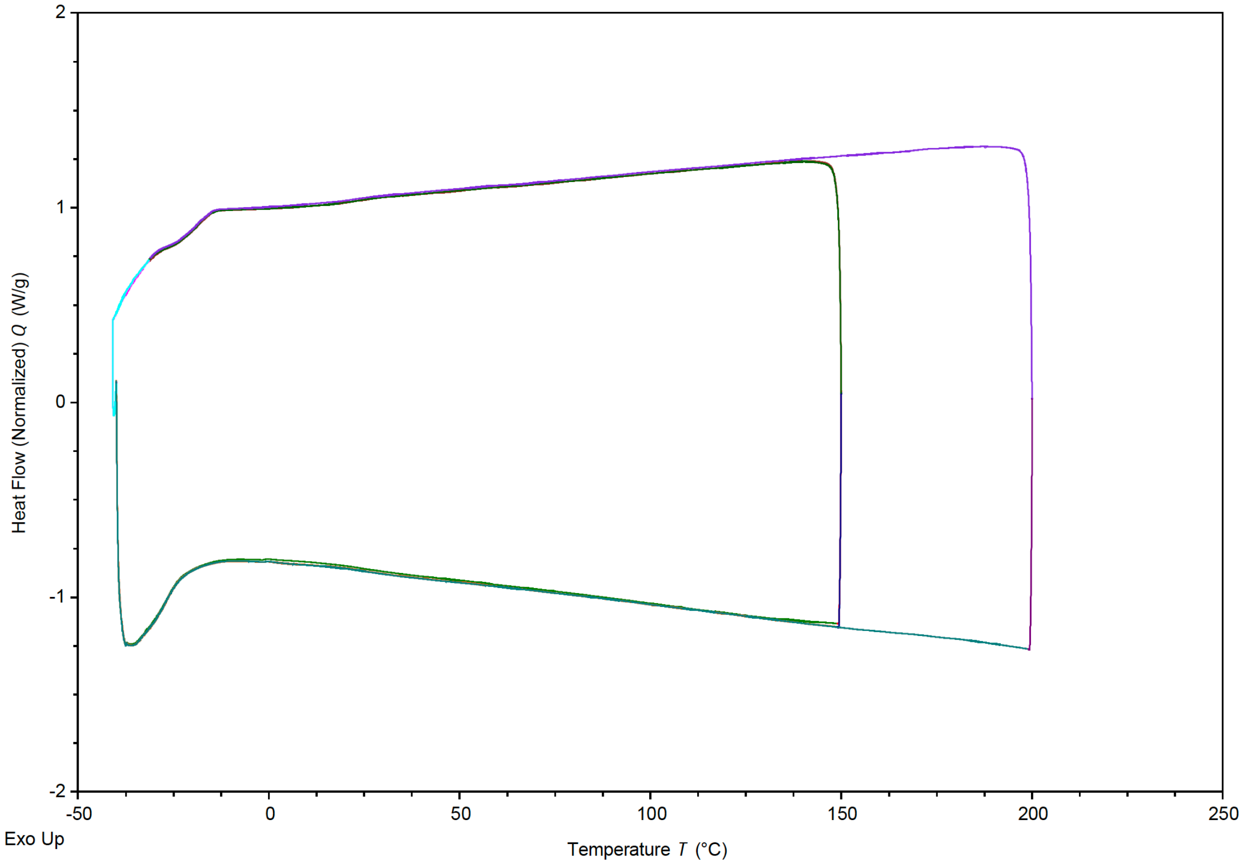

Figure S19: Thermal properties of the [$Co(HIm)_6$][NTf_2]$_2$ MIL measured as a function of temperature using DSC.

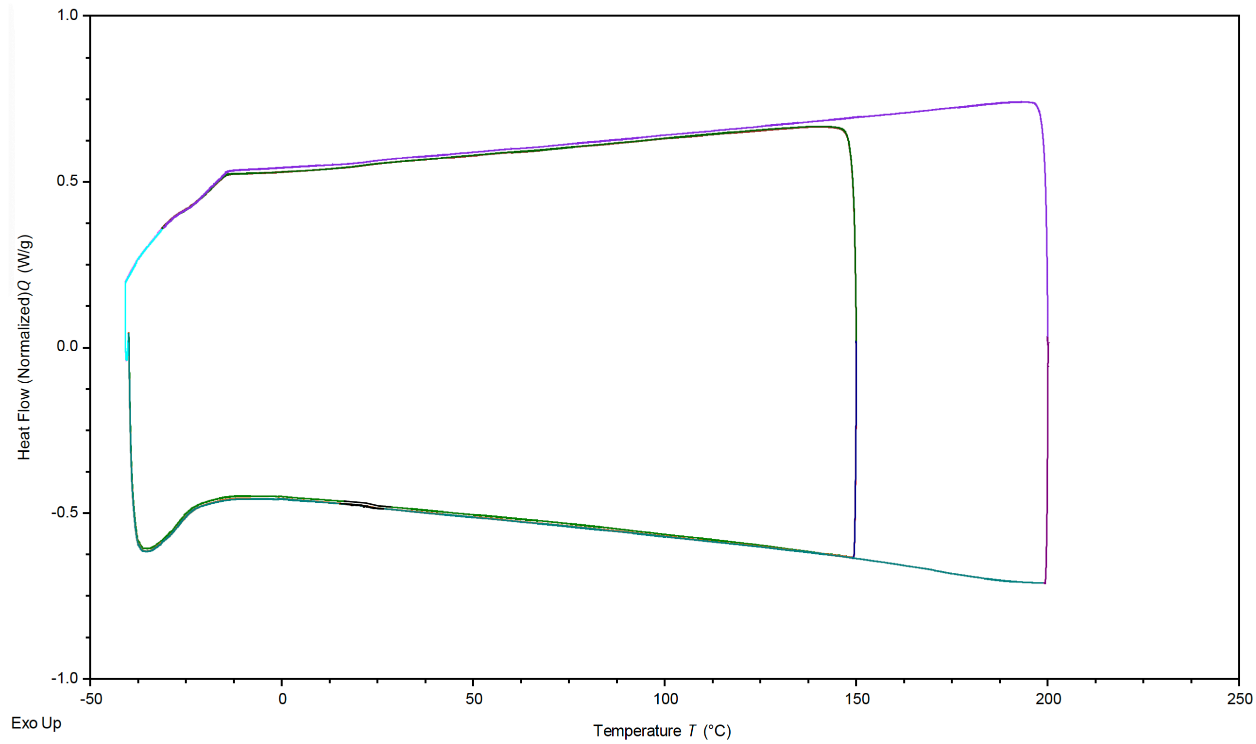

Figure S20: Thermal properties of the $[Ni(HIm)_6][NTf_2]_2$ MIL measured as a function of temperature using DSC.

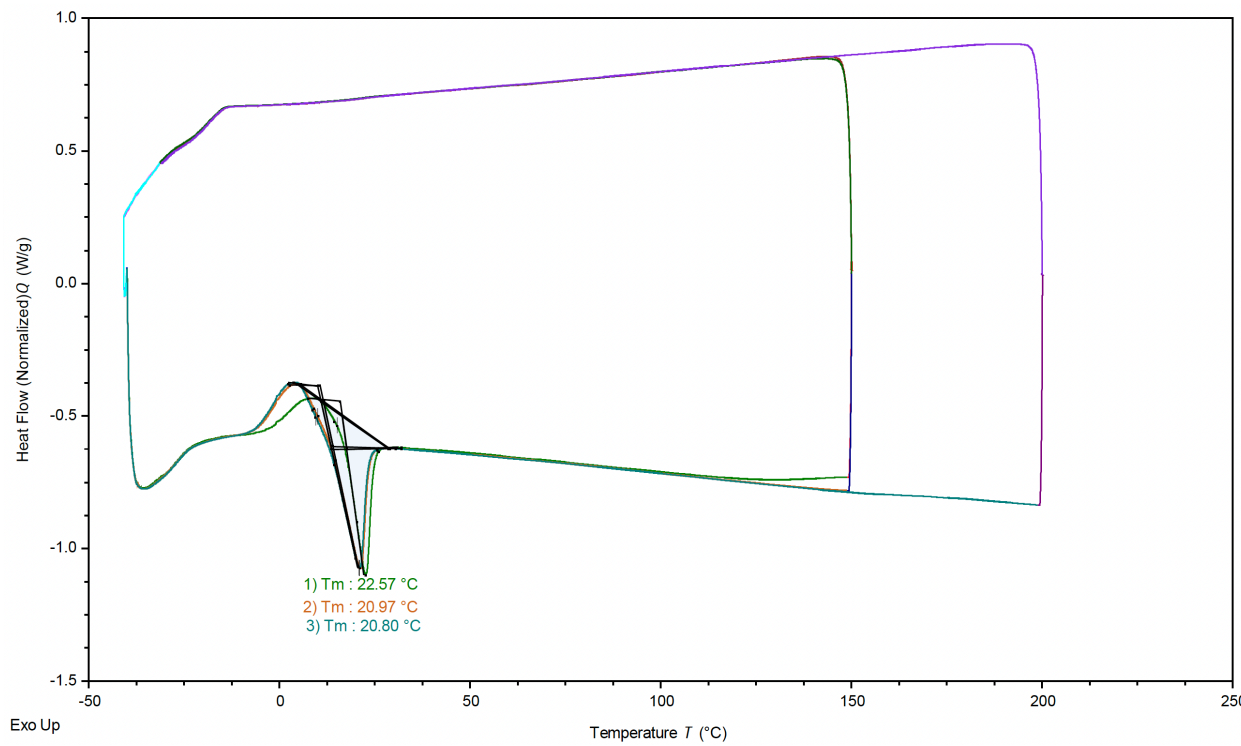

Figure S21: Thermal properties of the $[Co(OIm)_6][NTf_2]_2$ MIL measured as a function of temperature using DSC.

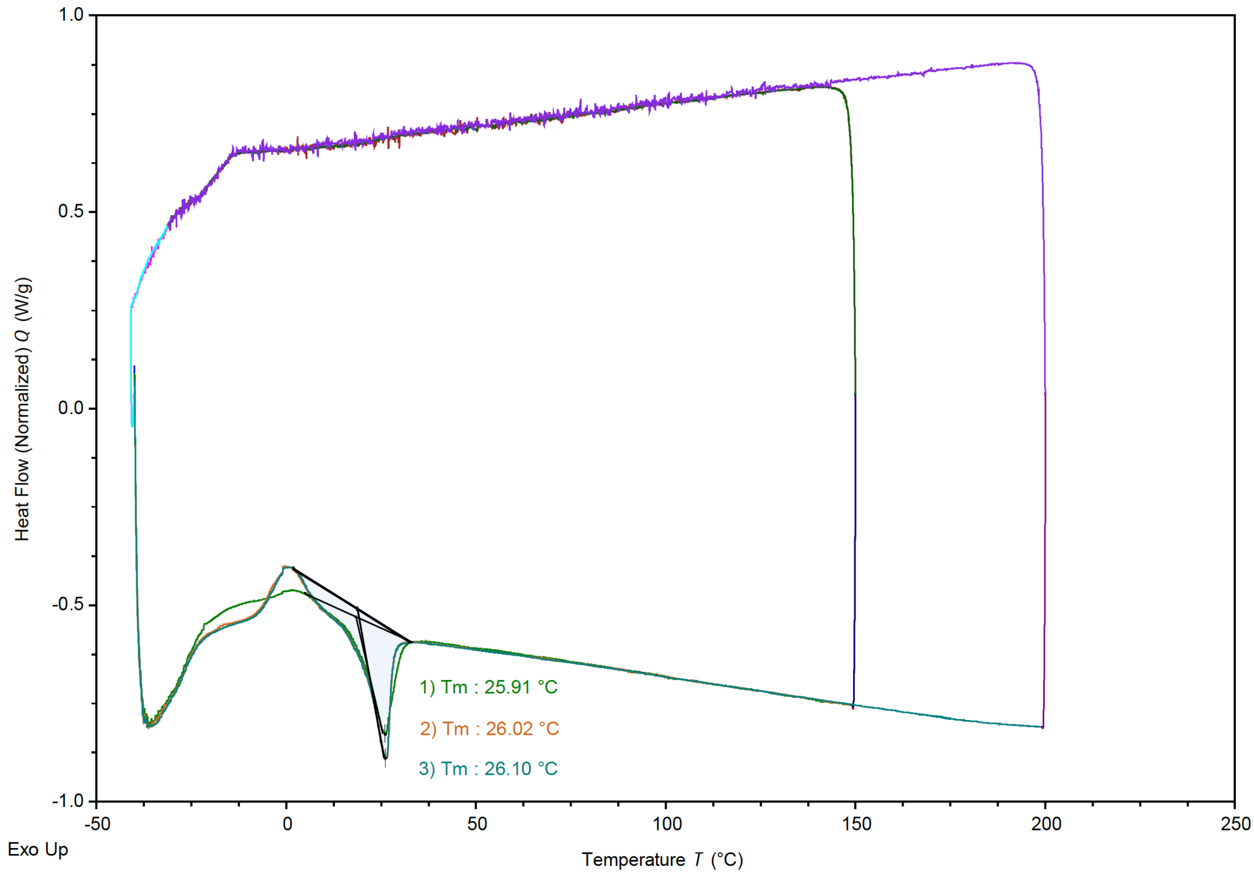

Figure S22: Thermal properties of the [Ni(OIm)$_6$][NTf$_2$]$_2$ MIL measured as a function of temperature using DSC.

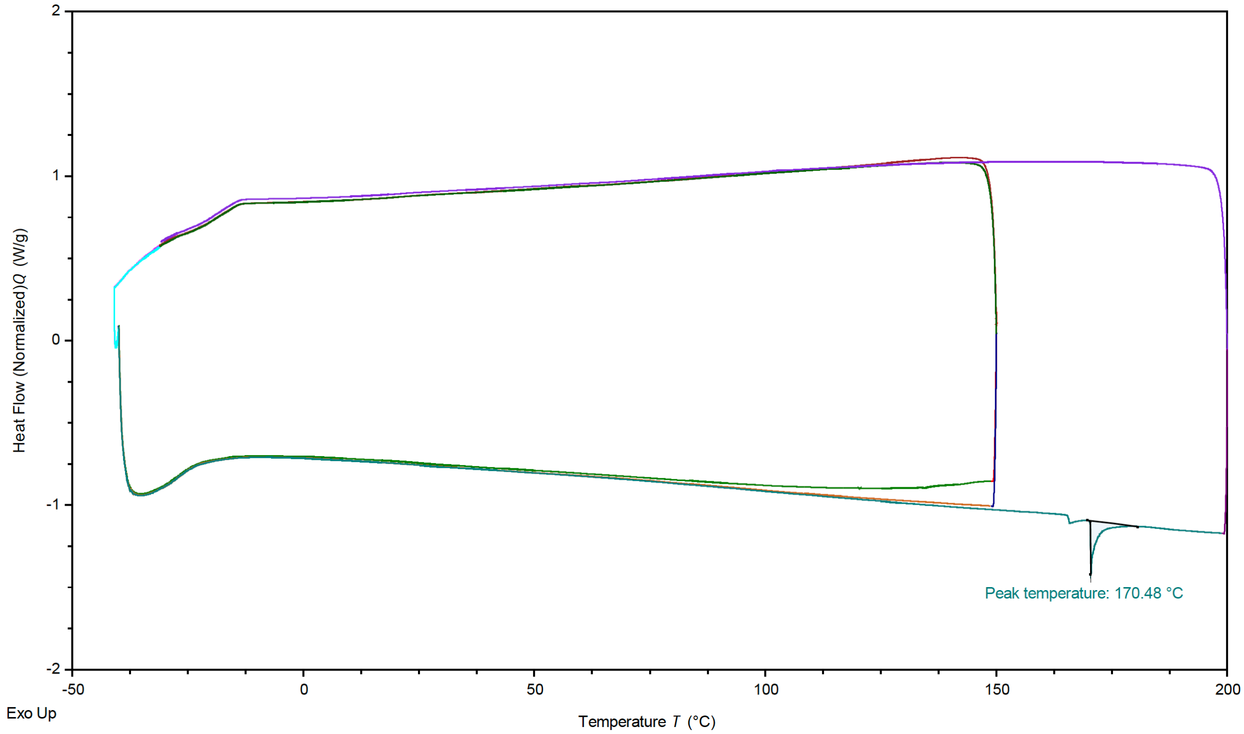

Figure S23: Thermal properties of the $[Co(AmIm)_6][NTf_2]_2$ MIL measured as a function of temperature using DSC.

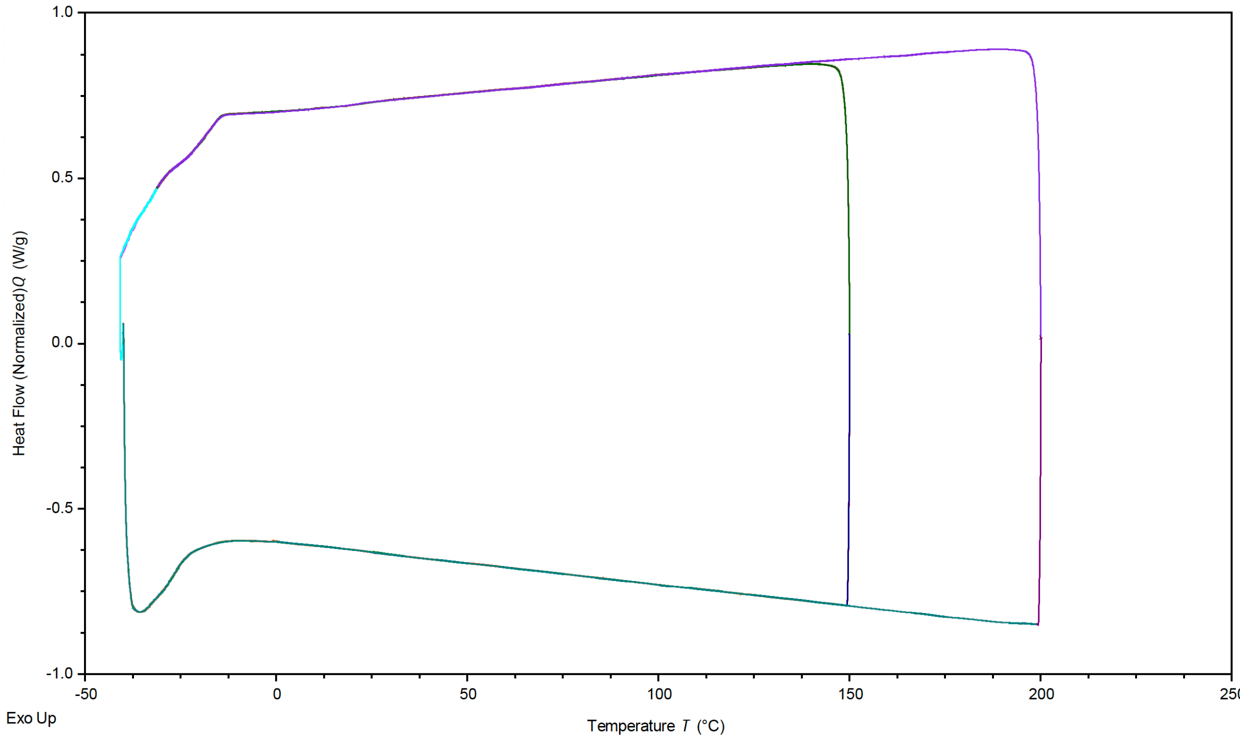

Figure S24: Thermal properties of the $[Ni(AmIm)_6][NTf_2]_2$ MIL measured as a function of temperature using DSC.

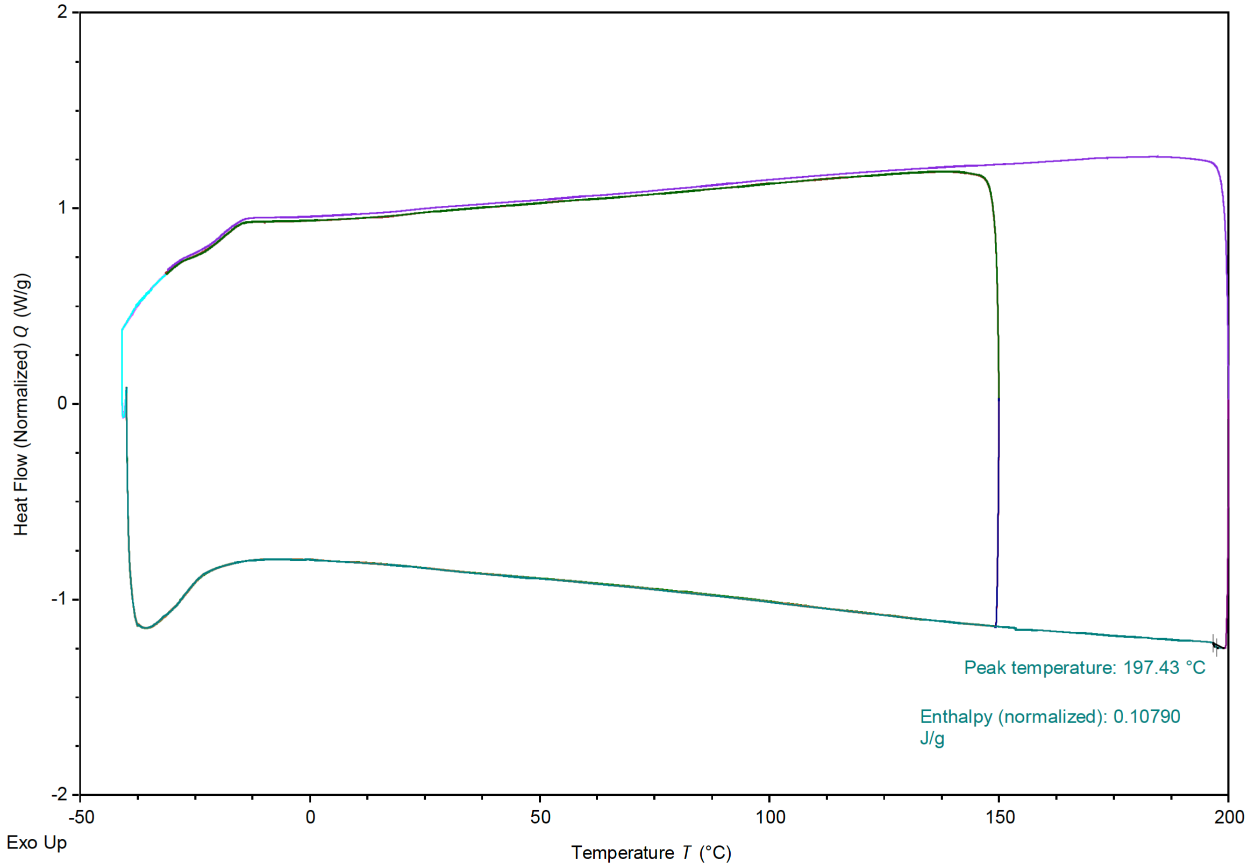

Figure S25: Thermal properties of the [Co(*N*,*N*-DMAc)$_6$][NTf_2]$_2$ MIL measured as a function of temperature using DSC.

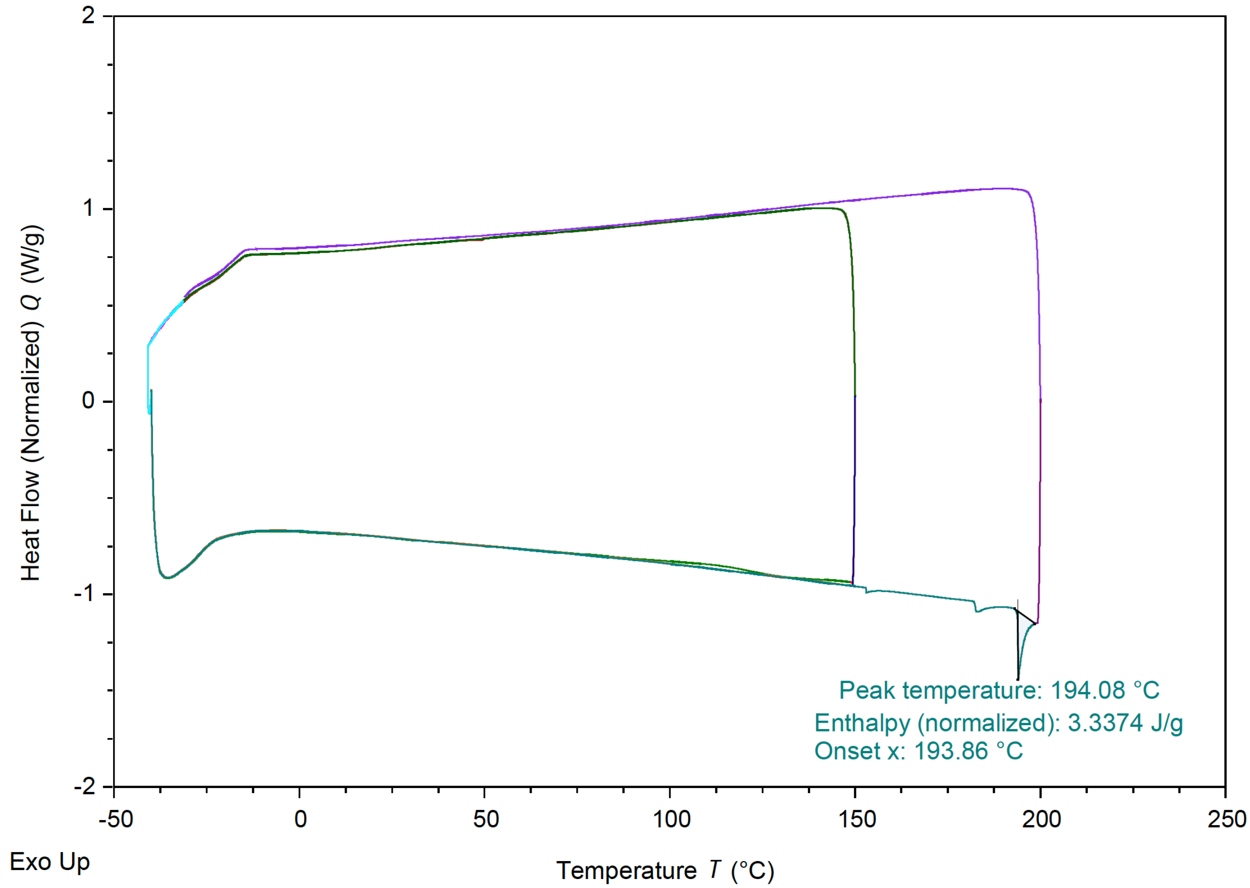

Figure S26: Thermal properties of the $[Ni(N,N\text{-}DMAc)_6][NTf_2]_2$ MIL measured as a function of temperature using DSC.

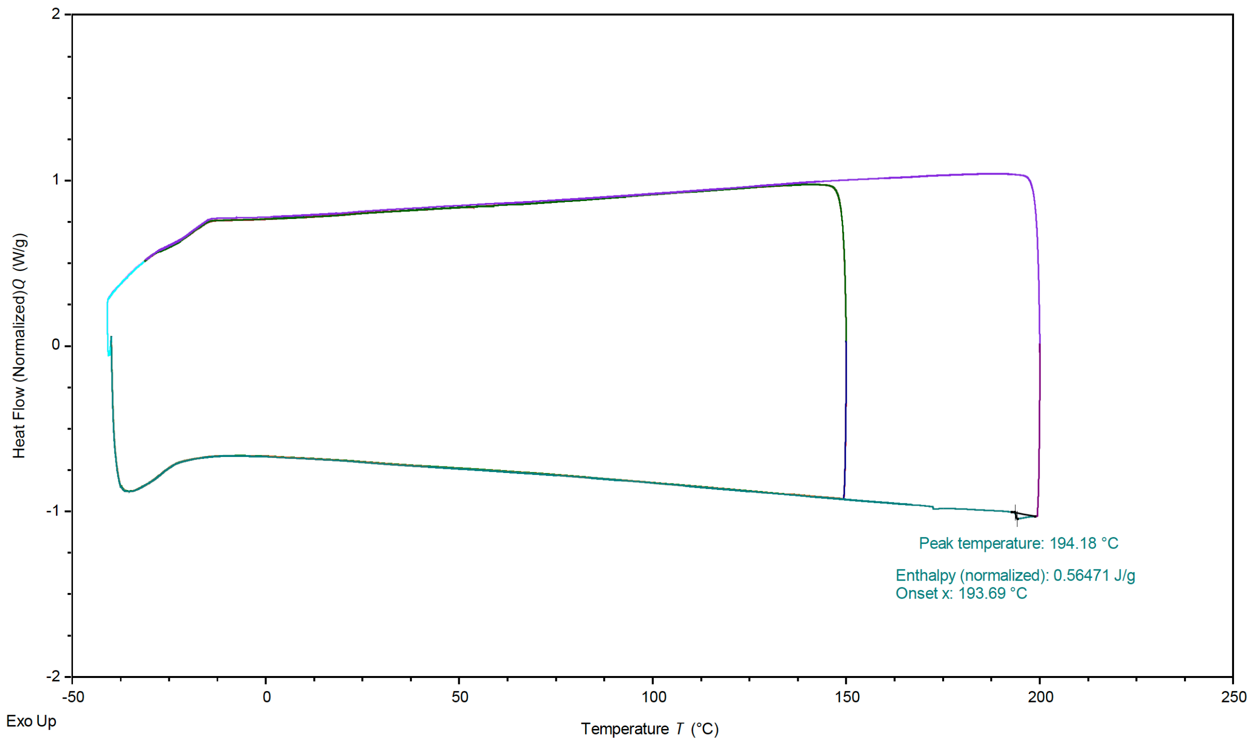

Figure S27: Thermal properties of the [Co(*N*,*N*-DMP)$_6$][NTf$_2$]$_2$ MIL measured as a function of temperature using DSC.

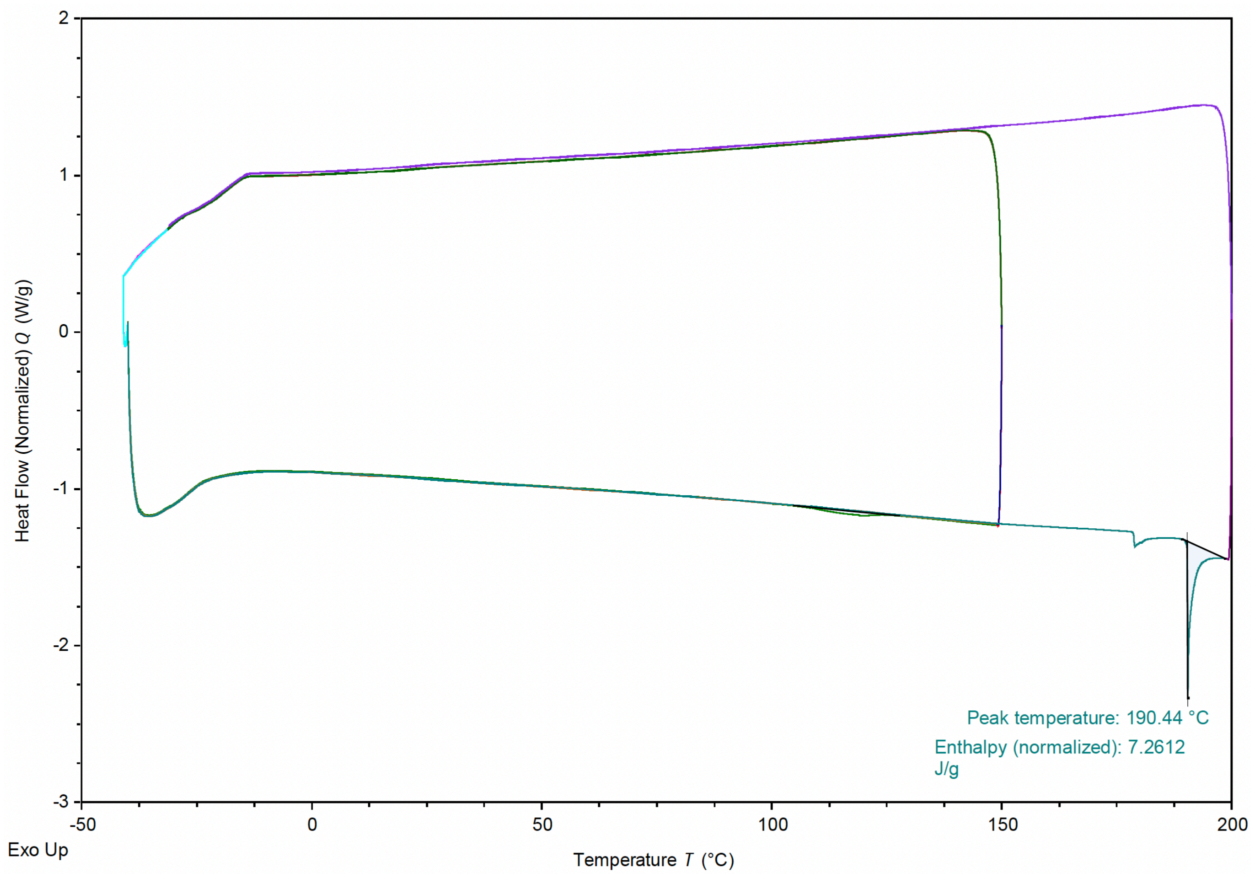

Figure S28: Thermal properties of the $[Ni(N,N\text{-DMP})_6][NTf_2]_2$ MIL measured as a function of temperature using DSC.

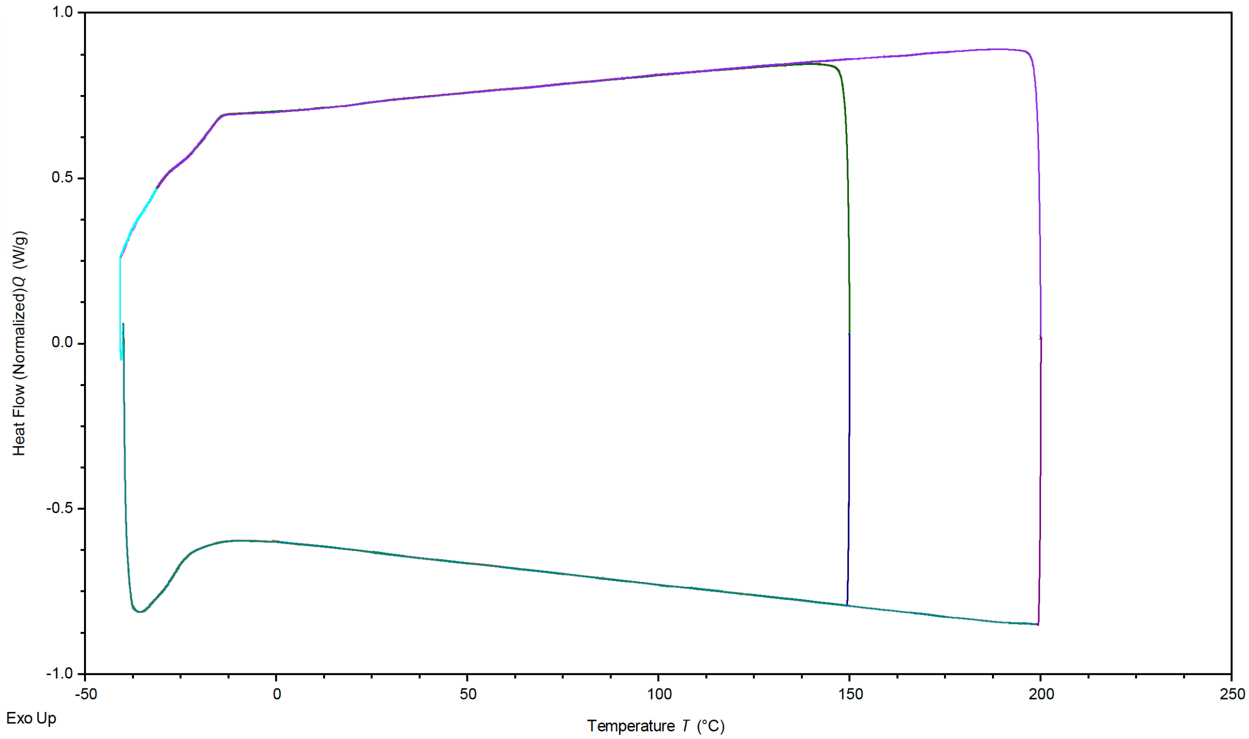

Figure S29: Thermal properties of the $[Co(TODGA)_2][NTf_2]_2$ MIL measured as a function of temperature using DSC.

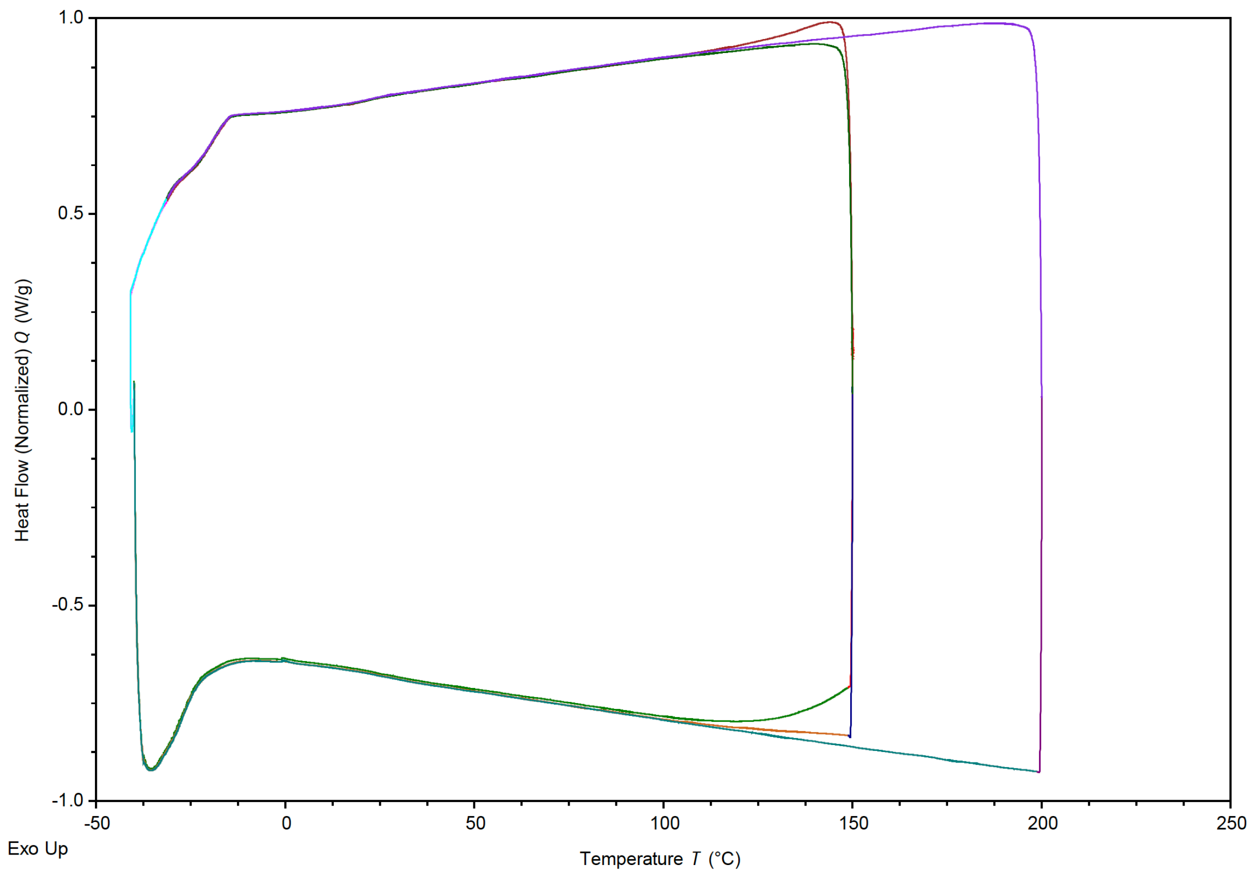

Figure S30: Thermal properties of the $[Co(TODGA)_2][NTf_2]_2$ MIL measured as a function of temperature using DSC.

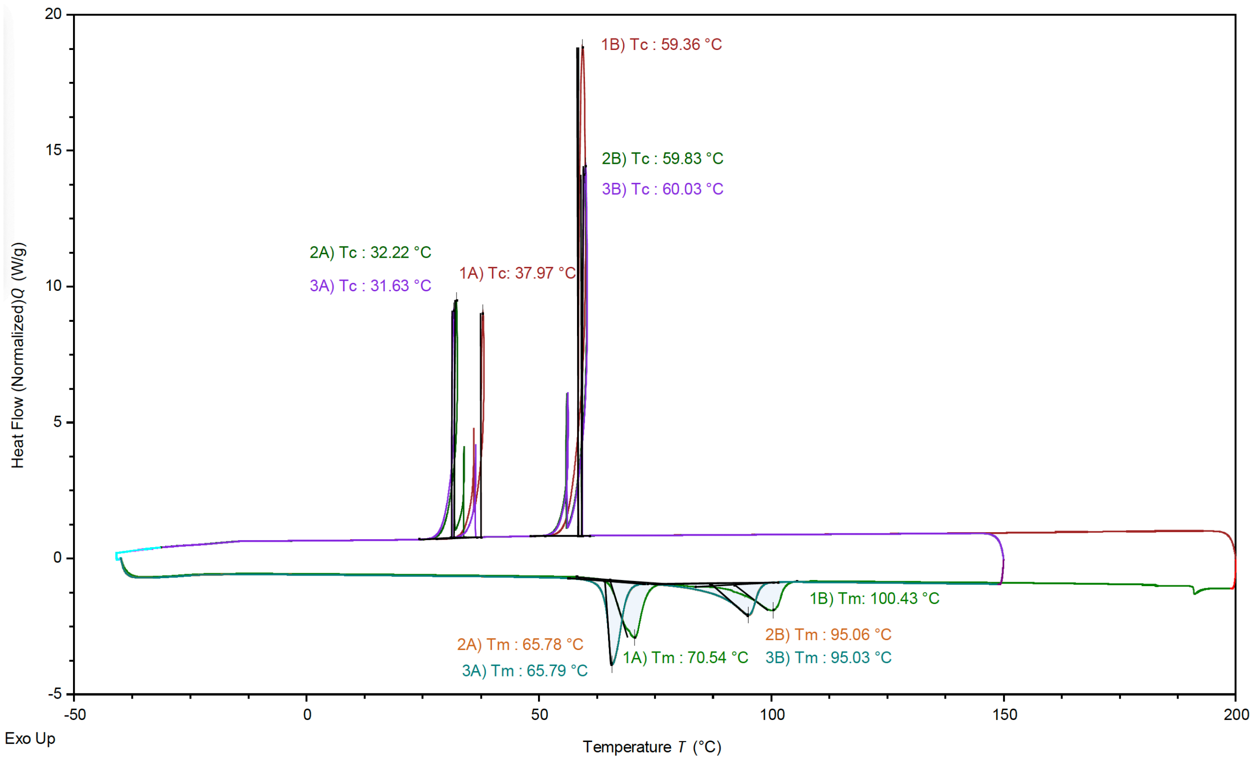

Figure S31: Thermal properties of the $[Co(H_2O)_6][NTf_2]_2$ salt measured as a function of temperature using DSC.

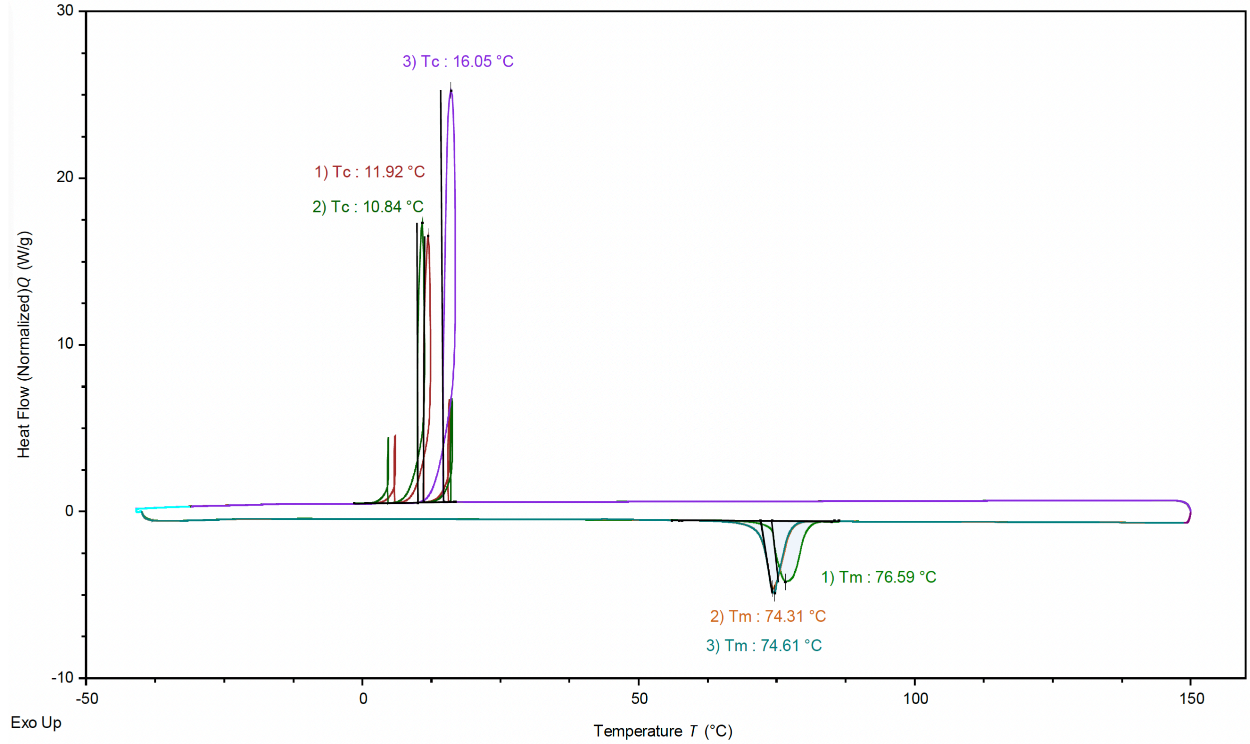

Figure S32: Thermal properties of the $[Ni(H_2O)_6][NTf_2]_2$ salt measured as a function of temperature using DSC.

^{1}H NMR of *N*,*N*,*N'*,*N'*-tetraoctyl diglycolamide (TODGA)

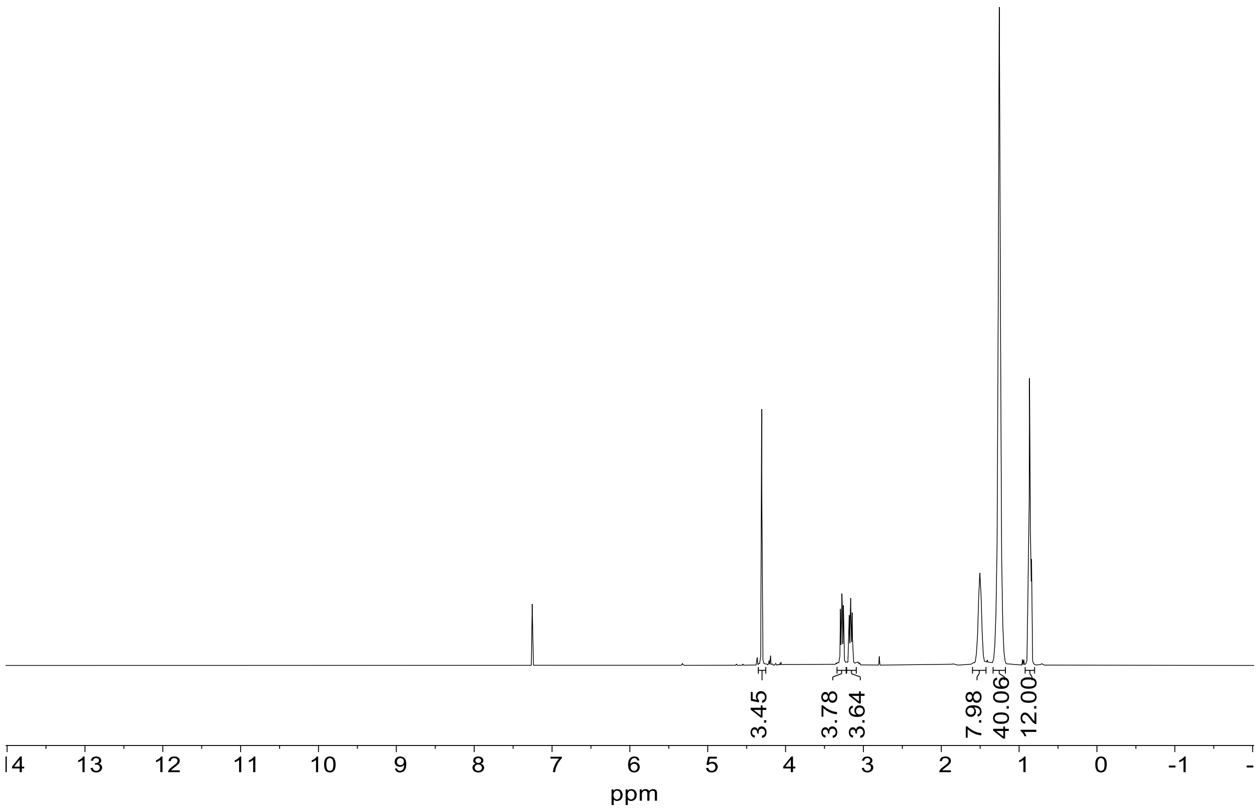

^{1}H NMR (400 MHz, cdcl$_3$) δ 4.31 (s, 3H), 3.34 – 3.22 (m, 4H), 3.22 – 3.09 (m, 4H), 1.60 – 1.43 (m, 8H), 1.33 – 1.18 (m, 40H), 0.86 (td, *J* = 6.8, 3.3 Hz, 12H).

[13]C NMR of *N,N,N',N'*-tetraoctyl diglycolamide (TODGA)

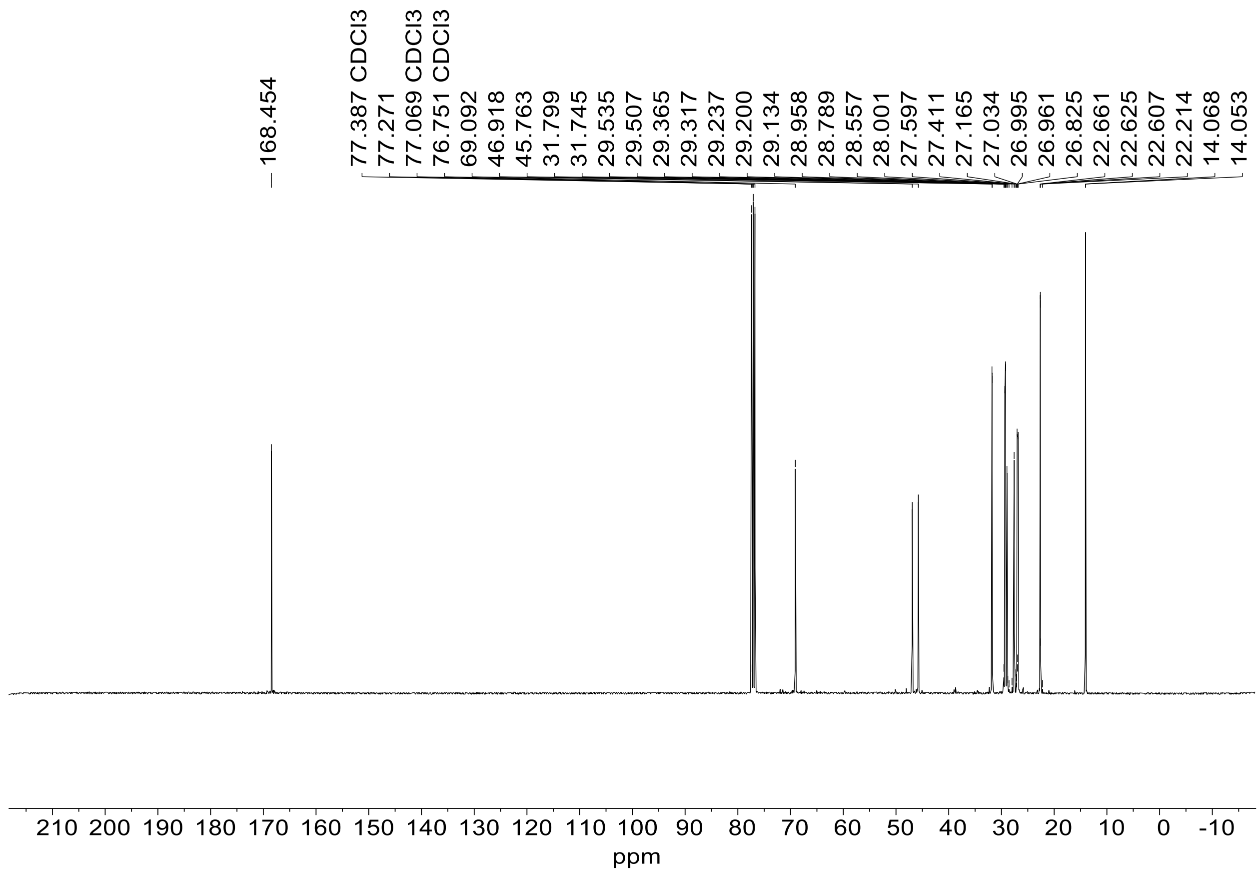

[13]C NMR (101 MHz, $CDCl_3$) δ 168.45, 77.27, 69.09, 46.92, 45.76, 31.80, 31.75, 29.51, 29.36, 29.32, 29.24, 29.20, 28.96, 28.79, 27.60, 27.41, 27.16, 27.03, 26.99, 26.96, 26.82, 22.66, 22.63, 22.61, 14.07, 14.05.

References

(1) Nacham, O.; Clark, K. D.; Yu, H.; Anderson, J. L. Synthetic Strategies for Tailoring the Physicochemical and Magnetic Properties of Hydrophobic Magnetic Ionic Liquids. *Chem. Mater.* **2015**, *27* (3), 923–931. https://doi.org/10.1021/cm504202v.